









Short-term variation in leaf-level water use efficiency in a tropical forest

Kenneth J. Davidson^{1,2} , Julien Lamour¹ , Alistair Rogers¹ , Kim S. Ely¹ , Qianyu Li¹ ,
Nate G. McDowell^{3,4} , Alexandria L. Pivovarov⁵ , Brett T. Wolfe^{6,7} , S. Joseph Wright⁷ ,
Alfonso Zambrano⁷  and Shawn P. Serbin¹ 

¹Department of Environmental and Climate Sciences, Brookhaven National Laboratory, Building 490A, Upton, NY 11973, USA; ²Department of Ecology and Evolution, Stony Brook University, 650 Life Sciences Building, Stony Brook, NY 11794, USA; ³Atmospheric Sciences and Global Change Division, Pacific Northwest National Laboratory, PO Box 999, Richland, WA 99352, USA; ⁴School of Biological Sciences, Washington State University, PO Box 644236, Pullman, WA 99164-4236, USA; ⁵Biology Division, Glendale Community College, 1500 N Verdugo Rd, Glendale, CA 91208, USA; ⁶School of Renewable Natural Resources, Louisiana State University, Room 227, Renewable Natural Resources Bldg, Baton Rouge, LA 70803, USA; ⁷Smithsonian Tropical Research Institute, Apartado, 0843-03092 Balboa, Panama

Summary

Author for correspondence:

Kenneth J. Davidson

Email: kdavidson.sci@gmail.com

Received: 28 September 2022

Accepted: 13 December 2022

New Phytologist (2023) **237**: 2069–2087

doi: 10.1111/nph.18684

Key words: climate model, diurnal response, leaf phenology, sap flux, stomatal conductance, stomatal optimization, transpiration, water use efficiency (WUE).

- The representation of stomatal regulation of transpiration and CO₂ assimilation is key to forecasting terrestrial ecosystem responses to global change. Given its importance in determining the relationship between forest productivity and climate, accurate and mechanistic model representation of the relationship between stomatal conductance (g_s) and assimilation is crucial.
- We assess possible physiological and mechanistic controls on the estimation of the g_1 (stomatal slope, inversely proportional to water use efficiency) and g_0 (stomatal intercept) parameters, using diurnal gas exchange surveys and leaf-level response curves of six tropical broadleaf evergreen tree species.
- g_1 estimated from *ex situ* response curves averaged 50% less than g_1 estimated from survey data. While g_0 and g_1 varied between leaves of different phenological stages, the trend was not consistent among species. We identified a diurnal trend associated with g_1 and g_0 that significantly improved model projections of diurnal trends in transpiration.
- The accuracy of modeled g_s can be improved by accounting for variation in stomatal behavior across diurnal periods, and between measurement approaches, rather than focusing on phenological variation in stomatal behavior. Additional investigation into the primary mechanisms responsible for diurnal variation in g_1 will be required to account for this phenomenon in land-surface models.

Introduction

Properly parameterizing Earth system models (ESMs) is of vital importance to forecasting terrestrial ecosystems' responses to novel future climates (Rogers *et al.*, 2017). In particular, the ESM representation of the terrestrial biosphere in land-surface models (LSMs) used to predict the dynamics, responses, and feedbacks of vegetation to the climate system is a critical requirement for climate modeling (Bonan, 2008). This includes the representation of photosynthetic carbon assimilation (A), which directly determines ecosystem net carbon uptake (Ainsworth & Rogers, 2007). Transpiration (E), which is a dominant flux in the hydrologic cycle (Schlesinger & Jasechko, 2014), is fundamentally governed by stomatal conductance (g_s), which regulates both A and E (Meidner & Mansfield, 1968; Hetherington & Woodward, 2003; Lawson & Vialet-Chabrand, 2019). Despite the large influence of g_s on global carbon and water cycles, parametrization of g_s in models remains one of the largest

uncertainties in current predictions of net ecosystem productivity (Bauerle *et al.*, 2014; Dietze *et al.*, 2014; Jefferson *et al.*, 2017; Franks *et al.*, 2018; Ricciuto *et al.*, 2018).

The LSMs that are commonly used in ESMs tend to represent g_s using an assumed linear relationship between g_s and A where the slope parameter governs the ratio of $g_s : A$ (Damour *et al.*, 2010). The majority of these formulations are phenomenological (e.g. Wong *et al.*, 1979; Farquhar & Wong, 1984; Ball *et al.*, 1987; Leuning, 1995; Damour *et al.*, 2010); however, Medlyn *et al.* (2011) argued that the relationship could be modeled in terms of stomatal optimality theory. The principal of stomatal optimization is that the evolution of vascular plants has prioritized maximizing A , per unit of water lost via E (Cowan & Fraquhar, 1977; Cowan, 1978). Stated in terms of water, stomatal regulation should minimize g_s so that E is minimized for a given amount of A , at least during periods of water limitation. This is mathematically represented by $\partial E/\partial A = \lambda$, where $1/\lambda$ represents the whole plant water use efficiency (WUE). This

relationship is conceptualized in the 'Unified Stomatal Optimization model' (USO; Medlyn *et al.*, 2011; Eqn 1).

$$g_s = g_0 + 1.6 \left(1 + \frac{g_1}{\sqrt{D}} \right) \frac{A}{C_s} \quad \text{Eqn 1}$$

Unlike phenomenological models, the g_1 term in the USO model relates directly to optimality theory (Cowan & Fraughar, 1977; Cowan, 1978). The stomatal slope term (g_1) is approximately inversely proportional to WUE. The stomatal intercept (g_0) is the expected g_s when net assimilation ($A_{\text{net}} = 0$) and occurs at an irradiance level equivalent to the light compensation point. The g_0 parameter was an empirical addition and intended to help constrain the model and ensure predicted g_s is always positive, rather than a feature predicted by optimality (Duursma *et al.*, 2019). The other terms in the USO model relate to environmental conditions, including the leaf-to-air vapor pressure deficit (D) and the CO_2 concentration at the leaf surface (C_s). Previously, Wu *et al.* (2019b) tested four different stomatal model formulations in the wet tropics and found that the USO model was best suited to represent g_s in this system.

Data used to fit the USO model can be collected either by taking survey measurements at ambient conditions (Bernacchi *et al.*, 2006; Lin *et al.*, 2015; Wu *et al.*, 2019b) or by the use of a response curve method (Ball *et al.*, 1987; Leuning, 1995; Leakey *et al.*, 2006; Domingues *et al.*, 2014; Wolz *et al.*, 2017; Davidson *et al.*, 2022; Lamour *et al.*, 2022b). In the survey method, *in situ* measurements of instantaneous gas exchange from many individual leaves are collectively used to fit a regression from which g_1 and g_0 are obtained. In the curve method, slow irradiance, vapor pressure deficit (VPD), or CO_2 response curves are used to illicit stomatal response, usually on a cut branch segment. For this approach, it is typical to calculate g_0 and g_1 for an individual leaf.

Much of the work to date on assessing variation of stomatal parameters has focused on specific biotic or abiotic drivers. Research into the effects of drought, soil moisture (Hérault *et al.*, 2013), and temperature (Lin *et al.*, 2015; Wolz *et al.*, 2017) has shown that, in some systems, the abiotic control on g_1 may be stronger than any biotic controls (Zhou *et al.*, 2014, 2016). Other work has linked leaf phenology and photosynthetic properties in tropical evergreen forests, where the rate of leaf production and leaf longevity both influence leaf function (van Schaik *et al.*, 1993). Leaves with longer average lifespans have reduced maximum carboxylation rate of the enzyme Rubisco (V_{cmax}) as compared to shorter lived leaves (Kitajima *et al.*, 1997, 2002). Similarly, Wu *et al.* (2016) found that V_{cmax} changed over the lifetime of tropical leaves, and this leaf-age variation is an important factor to consider when modeling tropical forest carbon assimilation (Wu *et al.*, 2017). Yet, it remains to be seen what impact leaf phenology has on stomatal parameters in tropical species. A strong phenological partitioning of leaf-level stomatal response, if it occurs, would most likely be an important development for ESMs given the large impact phenology has on terrestrial carbon dynamics (De Weirdt *et al.*, 2012). This is especially true for evergreen tropical forests, where leaves are found across a particularly wide range of phenological stages and where

phenological changes drive a large variation in seasonal carbon uptake (Wu *et al.*, 2016, 2017).

Other research has focused on the temporal consistency of stomatal parameters (Resco de Dios *et al.*, 2020), or the conditions in which the g_s response should be optimized (Katul *et al.*, 2010). Plants may optimize their stomatal operation across a variety of time scales, from near instantaneous response to stimuli such as sunflecks (Way & Pearcy, 2012; Company *et al.*, 2016), diurnal responses such as those to drying soil (Knapp, 1993; Zhang *et al.*, 2018), and long-term responses such as those which optimize water and nutrient uptake by roots (Franklin, 2007). Thus, whole plant WUE is the integration of all these factors, with leaf-level WUE lying at the end of a hierarchy of responses (Katul *et al.*, 2010). Wu *et al.* (2019b) addressed the seasonal consistency of tropical WUE by analyzing dynamics of g_1 during a drought event and found that species-specific g_1 did not significantly vary by month, suggesting that at the whole canopy-scale WUE is stable through time. However, the diurnal consistency of leaf-level WUE in this system remains untested. If they occur, diurnal adjustments in WUE may be in response to rapidly changing external stimuli such as changes in VPD during the day (Katul *et al.*, 2009), or may be the consequence of shifting water supply and carbon demand dynamics within the leaf (Bonan *et al.*, 2014; Dewar *et al.*, 2018). Understanding the degree to which WUE varies diurnally, and the main mechanisms which regulate these diurnal changes, may be helpful in developing more representative and robust process-based models of g_s and E in tropical broadleaf evergreen forests.

In this study, we measured leaf gas exchange on six evergreen tropical tree species to identify key biotic and abiotic controls on stomatal parameters and WUE. We had four main objectives: (1) compare survey and *ex situ* response curve-derived g_0 and g_1 to assess whether these two commonly used approaches provide comparable estimates of the key parameters; (2) determine whether g_0 and g_1 vary with leaf phenological stage; (3) assess whether g_0 and g_1 vary over a diurnal period; and (4) conduct simulations within a simplified canopy-scale model to understand the impacts of parameterization on E , comparing our estimated flux to a model benchmark derived from sap flux measurements. By addressing these four objectives, our goal was to develop a more detailed process-based understanding of stomatal function in wet tropical forests and identify several key axes of biotic and abiotic variation, which could be targeted for further investigation.

Materials and Methods

Site and species description

Data collection occurred from 6 January to 23 March 2020, in the San Lorenzo Protected Forest (9°16'1.71"N, 79°58'28.27"W), on the Colón Province on the Republic of Panama's Caribbean coast (Fig. 1). The site is characterized as a wet lowland (130 m asl) tropical forest, with a mean annual temperature of 23.4°C and an average of 3330 mm of rainfall (Paton, 2020). We used a crane operated by the Smithsonian Tropical Research Institute (STRI) for canopy access. Six tree species were selected for study,

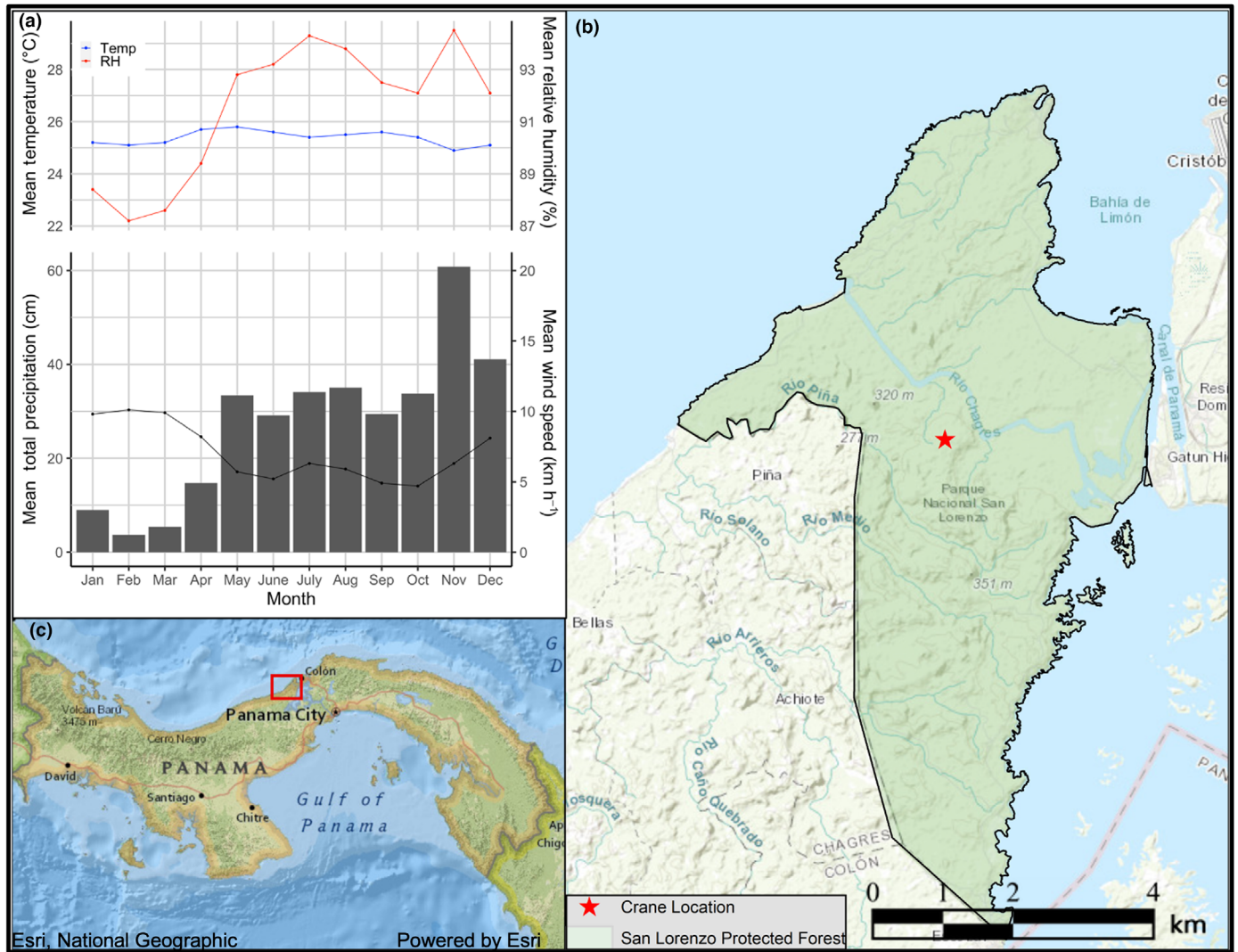


Fig. 1 Geographic location of the crane site (b) and the San Lorenzo Protected Forest (c) within the Isthmus of Panama, and (a) monthly climate averages collected at the site between 1997 and 2019. The period between January and April is considered the dry season, with less than 20% of annual rainfall (black bars). During the period of study, mean temperature was 25.5°C and mean daily precipitation was 1.3 mm.

chosen to span early, mid, and late successional growth strategies (Table 1). For each species, we sampled from two trees that were exposed to full sun throughout the day. Four of the trees had previously been instrumented for measurement of sap flux.

Gas exchange and leaf trait data collection

Gas exchange measurements were carried out using five LI-6400XT portable photosynthesis systems using a 6400-02(B) LED Light Source and an LI-6800 Portable Photosynthesis System using a Multiphase Flash Fluorometer leaf chamber (6800-01A; Li-Cor Biosciences, Lincoln NE, USA). For all measurements, the color spectrum of the irradiance was set to a fixed ratio of 90% red : 10% blue.

We used two different methods of gas exchange: an *ex situ* response curve approach and an *in situ* survey approach. Stomatal response curves on cut branch segments were carried out as described previously (Leakey *et al.*, 2006; Davidson *et al.*, 2022;

Lamour *et al.*, 2022b). Upper canopy, fully sun-exposed branches were cut predawn and immediately recut underwater to ease xylem tension and prevent embolism (Sperry, 2013). We recut a total of at least 50 cm back from the first cut to remove open vessels (Wolf *et al.*, 2016) with final branch lengths of *c.* 1.5 m. Cut branches were transferred in buckets to a shaded (*c.* 150 $\mu\text{mol PAR}$) location where all response curves were carried out. Each species was measured on 10–15 different days and spread across the duration of the field campaign. For each curve, irradiance level was reduced from saturating down to 0 $\mu\text{mol m}^{-2} \text{s}^{-1}$ photosynthetic photon flux density (PPFD) in a stepwise fashion every 20–40 min (Fig. 2a; Lamour *et al.*, 2022b). The irradiance value at saturation was derived for each species using photosynthetic response curves collected at multiple locations from across the top of each canopy (Lamour *et al.*, 2021b; Rogers *et al.*, 2022).

Survey measurements followed previous approaches (Rogers *et al.*, 2004; Wu *et al.*, 2019b). Fully sunlight top-of-canopy leaves were measured with the LI-6800. Before each

Table 1 Values for species-specific photosynthetic and conductance parameters and canopy scaling factors used in simulations of leaf-level A and g_s .

Species	$V_{max,25}$ ($\mu\text{mol m}^{-2} \text{s}^{-1}$)	$J_{max,25}$ ($\mu\text{mol m}^{-2} \text{s}^{-1}$)	$R_{dark,25}$ ($\mu\text{mol m}^{-2} \text{s}^{-1}$)	g_1 (kPa ^{0.5})	g_0 ($\text{mol m}^{-2} \text{s}^{-1}$)	DBH (cm)	LAI ($\text{m}^2 \text{m}^{-2}$)	Crown Area (m^2)	Sapwood area (m^2)	Successional status	Leaf lifespan (d)
<i>Brosimum utile</i> (Kunth) Oken	Young: 68.84	84.61	1.36	Response	0.013	–	–	–	–	Late	324
	Mature: 51.28	60.44	1.17	Curve: 2.40	0.029	–	–	–	–	–	–
	Old: 35.22	49.17	0.89	Survey: 3.04	–	–	–	–	–	–	–
<i>Cecropia insignis</i> Liebm.	Young: 77.48	109.48	1.50	Response	0.031	–	–	–	–	Early	231
	Mature: 78.70	108.48	1.81	Curve: 1.75	0.107	–	–	–	–	–	–
	Old: 60.50	89.33	1.68	Survey: 2.87	–	–	–	–	–	–	–
<i>Guatteria dumetorum</i> R. E. Fr.	Young: 38.66	65.71	1.24	Response	0.028	59.0	1.5	155.7	0.210	Mid	212
	Mature: 48.18	67.53	0.82	Curve: 1.96	0.067	–	–	–	–	–	–
	Old: 35.79	64.71	0.97	Survey: 3.32	–	–	–	–	–	–	–
<i>Miconia borealis</i> (Bonpl.) DC.	Young: 64.59	106.29	1.81	Response	0.034	34.0	1.15	74.42	0.080	Mid	189
	Mature: 71.60	108.38	0.92	Curve: 2.20	0.003	–	–	–	–	–	–
	Old: 54.06	94.55	0.79	Survey: 4.15	–	–	–	–	–	–	–
<i>Terminalia amazonia</i> (J.F. Gmel.) Exell	Young: 70.28	106.07	1.42	Response	0.022	52.9	1.5	134.57	0.174	Mid	160
	Mature: 77.85	116.16	1.14	Curve: 0.78	0.032	–	–	–	–	–	–
	Old: 51.34	87.52	1.24	Survey: 2.83	–	–	–	–	–	–	–
<i>Vochysia ferruginea</i> Mart.	Young: 46.57	76.14	1.67	Response	0.036	58.0	2.0	153.24	0.204	Mid	215
	Mature: 57.46	78.47	1.18	Curve: 0.67	0.040	–	–	–	–	–	–
	Old: 43.66	78.62	0.78	Survey: 2.57	–	–	–	–	–	–	–

For details regarding parameter estimates and tree functional traits, see section 'Canopy E simulations'. Data on leaf lifespan were previously reported in Osnas et al. (2018).

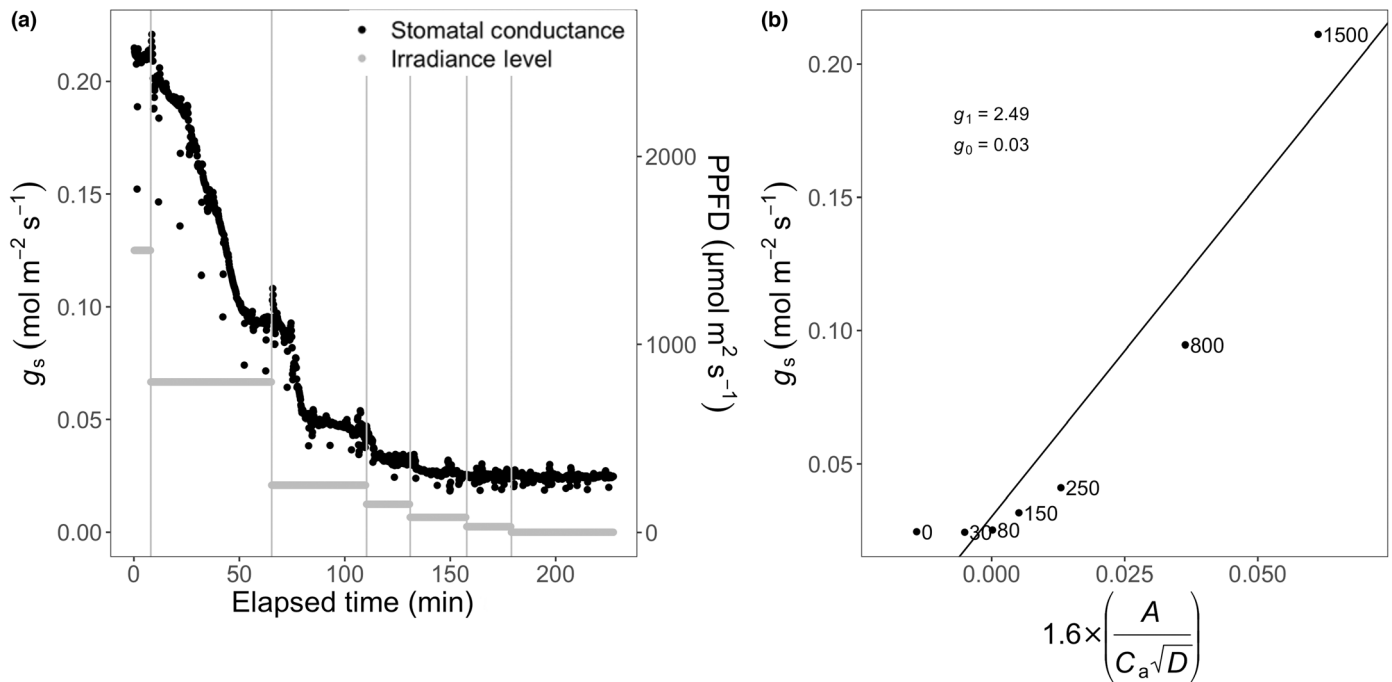


Fig. 2 Schematic representation of the response curve method. (a) Raw data from a response curve, with each black point representing an observation of stomatal conductance (g_s). At each irradiance level (horizontal grey bars), g_s drops then stabilizes, at which point irradiance is reduced to the next level (vertical grey bars). Across all irradiance levels, leaf temperature and vapor pressure at the leaf surface were held constant and close to ambient conditions. The CO_2 inside the leaf chamber was maintained at $400 \mu\text{mol mol}^{-1}$. (b) a typical regression fit of the points extracted from the seven irradiance levels, and the stomatal slope (g_1) and stomatal intercept (g_0) estimates produced from this curve. In this example, the nonlinearity of the response curve data, explored in detail by Lamour *et al.* (2022b), is readily apparent. For data analysis, many curves are combined to obtain one overall regression, with each curve acting as a random effect on the overall g_1 and g_0 estimates.

measurement, the conditions within the leaf chamber were set to match ambient air temperature ($22.8\text{--}32.6^\circ\text{C}$), CO_2 concentration ($c. 400 \text{ ppm}$), and irradiance ($3\text{--}2400 \mu\text{mol PAR}$). The relative humidity in the leaf chamber was maintained at 70% for all measurements, a level which allowed for VPD_{air} to be close to mean daytime conditions (Paton, 2020; Fig. S1), while minimizing condensation risk in the instrument. Each survey measurement consisted of a 30–90 s stabilization period, followed by five measurements of A and g_s at 5-s intervals, which were then averaged to produce a single data point.

Surveys were carried out from 06:30 h (approximate sunrise) to 18:30 h (approximate sunset) across eight different days. Two survey schemes were used, one in which we measured as many leaves as possible at three positions on a single tree crown for 40 min every hour for 4 h, and a second where each of the 12 tree crowns (two per species and three positions per tree) was measured as many times as possible for 12 min, replicating this pattern five times in a 12-h period. The aim of the first scheme was to assess the diurnal dynamics of a single species on a given day, while the aim of the second scheme was to broadly survey the forest. We used the data from the first scheme to parameterize our models (see Notes S1) and data from the second scheme, along with Wu *et al.* (2019b), to validate our models.

Immediately following the single species gas exchange survey measurements, the leaf was cut at the base of the petiole and stored in a humid, cool, dark box for further processing (Leach

et al., 1982; Rodriguez-Dominguez *et al.*, 2022). Processing included using a Scholander-type pressure chamber to measure leaf water potential (Ψ_{leaf} ; Scholander *et al.*, 1964). Following measurement of Ψ_{leaf} samples were dried to constant mass and weighed to determine leaf mass area (LMA; dry leaf mass per unit leaf area). Measured leaves were classified into one of three phenological stages, young, mature, or old (Table 1; Fig. 3).

Reflectance spectroscopy

We used a full-range spectroradiometer (PSR 3500+; Spectral Evolution Inc., Lawrence, MA, USA) together with an LC-RP-Pro leaf clip foreoptic (Spectra Vista Corp., Poughkeepsie, NY, USA) containing an internal, full-spectrum calibrated light source to measure leaf reflectance on all leaves following completion of stomatal response curves. The reflectance data were used to estimate $V_{\text{cmax},25}$ and $J_{\text{max},25}$ using the spectral methods and model presented in Lamour *et al.* (2021c).

Sap flux measurement

Sap flux velocity (cm s^{-1}) data were collected for four of the 12 study trees. Sap flux velocity was measured with Granier-type sensors (Model PS-TDP8; PlantSensors, Nakara, Australia), which use heat dissipation to empirically infer sap flux velocity (Granier, 1987). Each tree was instrumented with two sensors,

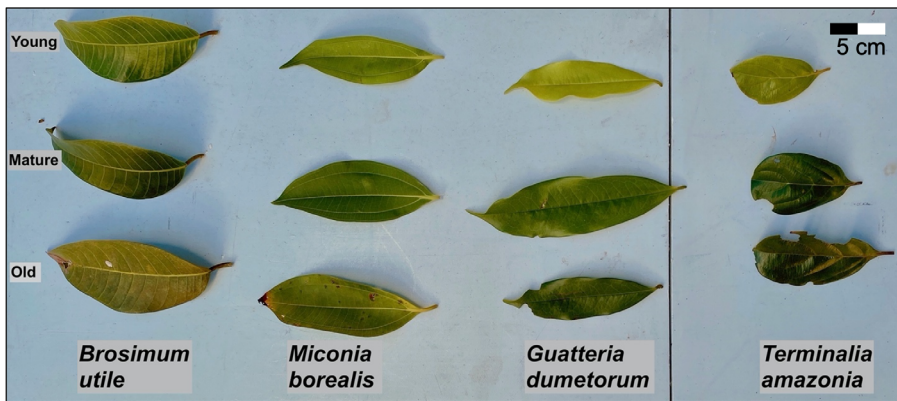


Fig. 3 Examples of the three phenological stages for four of the six species in this study. Young leaves were characterized as lighter in color, with minimal damage, softer more flexible texture, and a distal position on the branch. Mature leaves comprised the majority of the leaf material, characterized as fully expanded, having an intermediate color and texture as well as an intermediate position. Old leaves were very scarce for most species and tended to have minor surface damage, were dark in color, and were in extreme proximal positions on branches.

located at breast height, and positioned perpendicular to each other at a depth of 2 cm into the sapwood of the trees. Raw temperature data were processed in the R package AQUAFUX (v.1.0.0, Speckman, 2019) to derive sap flux velocity. Vapor pressure deficit data obtained on site from the STRI meteorological station were used to normalize minimum flux. Sap flux velocity data were multiplied by sapwood area (Meinzer *et al.*, 2001) to derive sap flow (g s^{-1}) at 15-min intervals, with the assumption that velocity was consistent across the sapwood radial profile. In total, there were 42 diurnal (05:30–18:30 h) periods of complete sap flux coverage for each of the four study trees during our period of study (Pivovarov *et al.*, 2020).

Estimation of conductance parameters

Stomatal response was evaluated using the USO model (Medlyn *et al.*, 2011; Fig. 2b; Eqn 1; Notes S1). g_1 represents the slope in the relationship shown in Eqn 2, a reconfiguration of Eqn 1 where g_1 directly acts as the slope between g_s and A , atmospheric CO_2 concentration (C_a), and VPD. The parameters g_1 and g_0 are mathematically identical in Eqns 1, 2 (Lamour *et al.*, 2022b); however, Eqn 2 provides for simpler graphical depiction of the data. Eqn 2 also uses C_a in place of C_s , as when using gas exchange systems, the terms are very similar (Lamour *et al.*, 2022c).

$$g_s - \frac{1.6 \times A}{C_a} = g_0 + g_1 \times \frac{1.6 \times A}{(\sqrt{D} \times C_a)}. \quad \text{Eqn 2}$$

As with any linear model, a limited range of measured g_s can affect the model fit by introducing uncertainty in the regression (g_1). The wider the range of the data, the lower the uncertainty in the fit of the model slope, assuming that the variation around the mean slope is consistent (e.g. no heteroscedasticity). For response curve data, we captured a full range of conductance values, as we are theoretically measuring g_s from its maximum (light saturated) value to its minimum (dark-adapted) value. A limited range of g_s can also lead to uncertainty in estimating a value for g_0 , especially if most measurements occurred far above the light compensation point. To keep analysis consistent between datasets, we chose to fit g_0 for the survey dataset rather than prescribe a value (Duursma *et al.*, 2019).

R_{dark} was calculated from dark-adapted measurements of A_{net} (the final response curve point) and was scaled to 25°C ($R_{\text{dark},25}$) using an inverse Arrhenius equation (Eqn 3; Bernacchi *et al.*, 2001; Von Caemmerer, 2013):

$$R_{\text{dark},25} = \frac{R_{\text{dark}}}{\exp\left(\frac{H_a}{(R \times T_{25})} - \frac{H_a}{(R \times T_{\text{leaf}})}\right)}. \quad \text{Eqn 3}$$

where H_a is the activation energy of mitochondrial respiration ($H_a = 46\,390 \text{ J mol}^{-1}$), and R is the ideal gas constant ($R = 8.314 \text{ J mol}^{-1} \text{ K}^{-1}$).

Canopy E simulations

As a method of evaluating the performance of different stomatal parameterizations against a benchmark data set, we modeled canopy-scale E response to ambient environmental conditions. We chose not to evaluate the model performance in simulating canopy scale A , as we have no benchmark which to compare model estimates. We used the R package LEAFGASEXCHANGE (v.1.0.1, Lamour & Serbin, 2021), which includes a coupled leaf scale steady state assimilation, conductance, energy balance, and radiation interception model. Details of model parameters and equations used can be found in Notes S2.

The model simulates environmental conditions around the leaf using local meteorological data (Paton, 2020). To simulate the radiation environment at the leaf surface, the model uses the radiation interception model developed by Norman (1979), which partitions incoming radiation into direct and diffuse streams. In each simulation, we assumed six canopy layers with a uniform distribution of leaf area index (LAI) between layers (Béland & Baldocchi, 2021). To simulate wind speed within the canopy we assumed an exponential decrease with LAI within the canopy following the model presented in equation 14 in Buckley *et al.* (2014). Values for $V_{\text{cmax},25}$, $J_{\text{max},25}$, $R_{\text{dark},25}$, g_0 , and g_1 , estimated as described previously, were averaged by species and by phenological stage (Table 1). In each model run, uncertainty was simulated by rerunning the model using g_1 and g_0 values corresponding to ± 1 SE of the fitted value.

Leaf-level estimates of E were scaled to the canopy by first summing across canopy layers and then multiplying by total

canopy area as estimated using the allometric function presented in Martínez Cano *et al.* (2019). Leaf area index estimates were made for each species (Condit *et al.*, 2013; Sirri *et al.*, 2019), which allow for an appropriate accounting of leaf area per ground area.

We then conducted a model simulation sensitivity analysis to explore the potential impacts of biotic variation on emergent, canopy scale E . To do this, we simulated different canopies with different combinations of leaf phenological classes, with leaf physiological properties based on leaf phenological stage. For this analysis, we assumed 'natural' conditions were a 15-80-5% partitioning between young, mature, and old leaves, an estimate that is in line with Wu *et al.* (2017). We compared our simulation results for canopy scale E with measured sap flow as a benchmark. Here, we expected that there was a delay between flux measured at the base of the tree and E in the canopy, so we averaged flux across a 15-min interval to minimize this discrepancy (Meinzer *et al.*, 2003).

Statistical analysis

To compare g_1 and g_0 estimates between tree species and phenological stages within tree species, we used mixed effects models constructed and analyzed in the R package NLME (v.3.1, Pinheiro *et al.*, 2020). For response curve data, the leaf served as the random effect, while for survey data, the location within the canopy of the tree served as the random effect. For all data, we considered the species and phenological stage as fixed effects. The equations and coefficients for the mixed models can be found in Notes S1 and Tables S1–S3.

To examine which of our three statistical models (response curve, survey, survey + time-of-day; Notes S1) predicts leaf-level g_s most accurately, we performed a validation of the fixed effects components of the models using two additional survey-derived datasets, one which was collected on four separate days during our 2020 field campaign (described above as scheme 2), and a second data set collected by Wu *et al.* (2019b) at the same site in 2016 (Rogers *et al.*, 2022). We then used validation statistics (r^2 , RMSE, likelihood ratio test) to determine which model predicted g_s most accurately.

We assessed the effect of species and species : leaf phenological stage on $V_{\text{cmax},25}$, $R_{\text{dark},25}$, and the effect of LMA, Ψ_{leaf} , and successional stage on g_1 and g_0 using ANOVA and *post hoc* Tukey tests. Finally, we compared canopy level transpiration simulations using ANOVA at the species level, and a *post hoc* Tukey's honest significant difference test to distinguish significance between factor levels. All analysis was performed using the R open-source software environment (v.3.6.2, R Core Team, 2013).

Results

Gas exchange dynamics of diurnal surveys and response curves

Here, we present the results from an analysis of 80 stomatal response curves (Fig. S2a) and 665 survey data points (Fig. 4;

Lamour *et al.*, 2021b). Both A and g_s respond strongly to the diurnal cycle of irradiance during the survey measurements (Fig. 4). VPD_{leaf} also exhibits a diurnal trend, peaking around solar noon, due to higher leaf temperatures, and a small increase in VPD_{air} (Fig. S1). Stomatal response curves can be used to examine potential maximum photosynthetic and stomatal fluxes. Here, we see that among species, there is significant variation in maximum g_s , with *Brosimum utile*, *Cecropia insignis*, and *M. borealis* having maximum g_s values up to three times that of the other three species (Fig. S2b).

We can compare the relationship between g_s and environmental conditions for both datasets (Fig. S2). We see that not only do the survey data have a larger overall range of conductance, there is also more within-species variation in conductance for a given set of environmental conditions. We can also see the nonlinearity of the response curve data, explored in detail by Lamour *et al.* (2022b), which is much less pronounced for the survey data set.

Model comparison and validation

We evaluated the accuracy of the models built on the different datasets (response curve, survey, and survey + time-of-day), first assessing their calibration scores, and then by predicting g_s measured by the survey method at the same site in 2016 (Rogers *et al.*, 2022) and using our 2020 validation dataset. In the calibration phase, the survey and survey + time-of-day models can be compared directly as they are derived using the same data set. The model including a time-of-day effect on g_1 and g_0 has an improved calibration r^2 (0.80 vs 0.75), a lower RMSE (0.0564 vs 0.0627 mol m⁻² s⁻¹), a lower AIC score (−1844 vs −1741), and a likelihood ratio test reveals the models were significantly different ($P < 0.001$). However, during the validation phase, the model calibrated on the survey dataset without a time-of-day effect performed the best, with the lowest RMSE, and the highest validation r^2 (Fig. 5).

g_1 values estimated using the response curve dataset were significantly ($P < 0.001$) lower than when they were estimated using the survey data set (Fig. 6). On average, the response curves produced estimates of g_1 which were 50% lower than estimates obtained from survey data. Only in the species *B. utile*, there was no significant difference in estimated g_1 (Fig. 6).

Finally, we simulated canopy scale E for all six species to compare how the different methods of deriving stomatal parameters perform in a modeling context at the larger whole-tree scale. Four of the six species also had scaled sap flux velocity measurements (Pivovarov *et al.*, 2020) to compare the modeled E allowing us to benchmark results (Fig. 7). We found that when comparing estimated and observed E , the survey + time-of-day parameterization had the lowest RMSE (0.013 g H₂O m⁻² s⁻¹) followed by survey (0.014 g H₂O m⁻² s⁻¹), and the response curve method (0.022 g H₂O m⁻² s⁻¹; Fig. S3). All three methods closely tracked changes in irradiance. However, the two survey methods captured the magnitude of the change in canopy E more closely than the response curve method (Fig. 7).

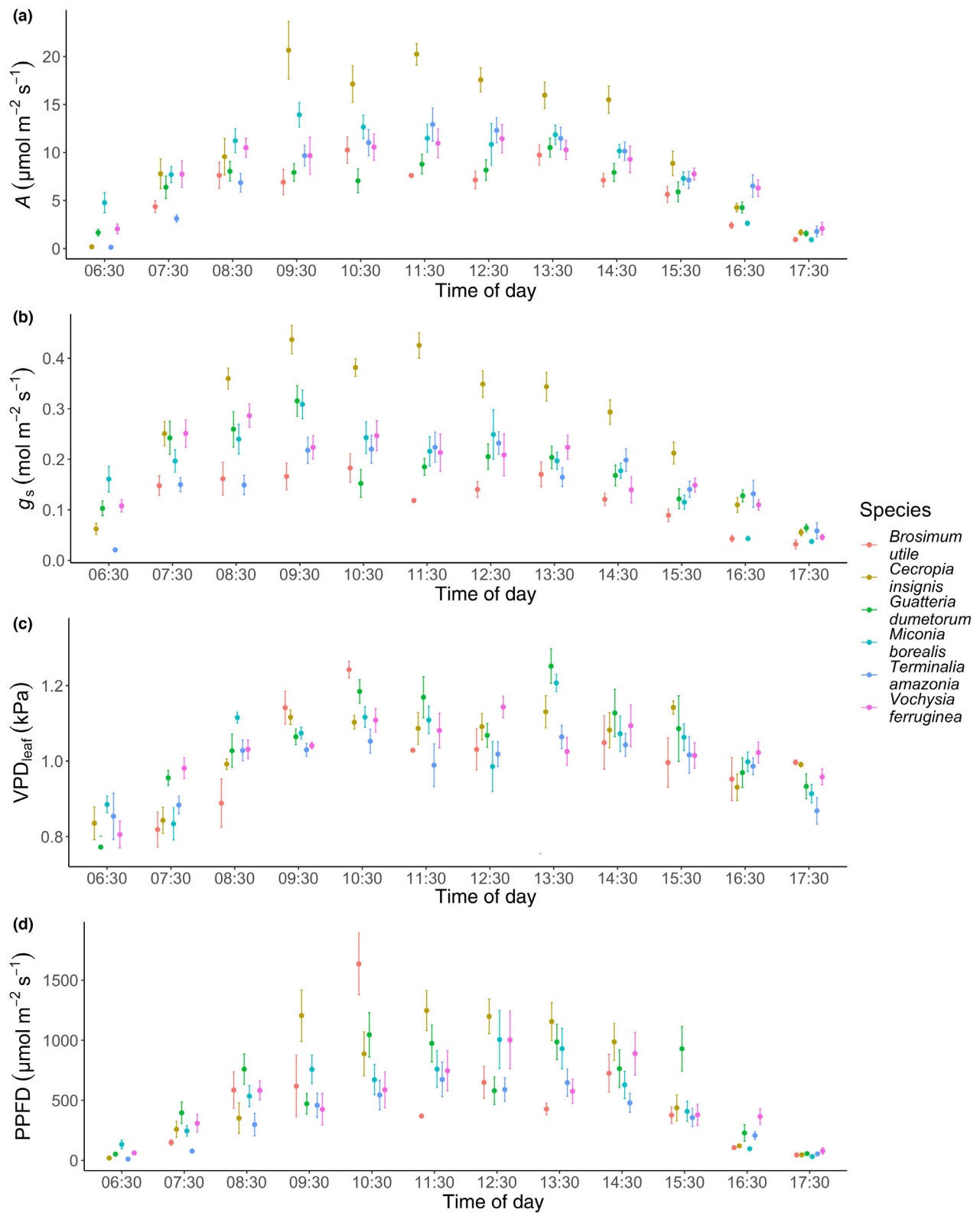


Fig. 4 Overview of leaf-level conditions observed during diurnal survey measurements. Species-specific averages of hourly (a) photosynthesis (A), (b) stomatal conductance (g_s), (c) vapor pressure deficit at the leaf surface (VPD_{leaf}), and (d) photosynthetic photon flux density (PPFD). Error bars represent ± 2 SE of the mean.

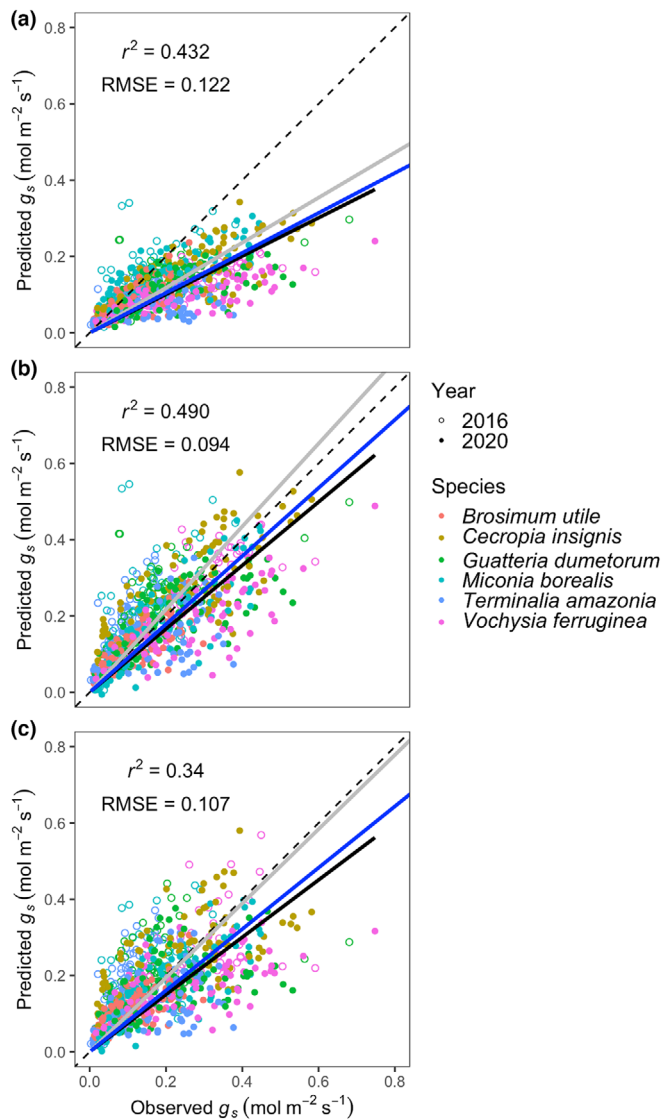


Fig. 5 Validation plots of observed values of leaf-level stomatal conductance (g_s) vs model predicted g_s . Data come from (a) the model based on response curve-derived stomatal intercept (g_0) and slope (g_1), (b) the model based on survey-derived g_0 and g_1 , and (c) the survey model with an inclusion of a time-of-day effect on g_1 . r^2 and root mean squared error (RMSE) values in each panel show that the survey model improves predictions of g_s over the response curve model; however, the inclusion of the time-of-day effect slightly worsens model predictive accuracy. Open circles were from the 2016 dataset collected by Wu *et al.* (2019b), while closed circles correspond to the 2020 validation data. Solid black, grey, and blue trend lines correspond to the lines of best fit for the 2016 data, 2020 data, and all the data, respectively. Dashed black line is a 1 : 1 reference line.

Effect of leaf phenological stage on estimated stomatal parameters

For the response curve data set, both g_1 and g_0 varied by tree species ($P < 0.001$) and phenological stage ($P = 0.009$) with a significant stage : species interaction ($P < 0.001$, Figs 8a, S4; Table 2). For the survey data set, g_0 varied by tree species ($P < 0.001$), phenological stage ($P < 0.001$) with a significant stage : species interaction ($P < 0.001$, Fig. S4; Table 2), but g_1 only varied among tree species ($P < 0.001$; Fig. 8b; Table 2).

When assessing the differences between the interactive effects of phenological stage and species on g_1 for response curves, we only found four significant effects: *B. utile* young and mature ($P = 0.003$, 66.9% decrease), *M. borealis* young and mature ($P = 0.006$, 61.2% decrease), *M. borealis* young and old ($P = 0.041$, 49.7% decrease), and *C. insignis* young and old ($P = 0.007$, 111% increase). We also used response curve data to investigate continuous relationships between g_0 and g_1 with other related leaf physiological traits, but did not observe a significant effect of LMA, Ψ_{leaf} or successional stage on g_1 or g_0 (Figs S5, S6).

Finally, we analyzed the interactive effects of phenological stage and species on $V_{cmax.25}$ and $R_{dark.25}$, derived from leaf spectroscopy. The relationships between stage and $R_{dark.25}$ ($P < 0.001$) and stage and $V_{cmax.25}$ ($P < 0.001$) were significant, c. 40% decrease in values between the mature and old phenological stages (Fig. S7; Table 1).

Investigation of a time-of-day effect

Using the survey dataset (Fig. 4), we tested whether the time-of-day influenced g_0 and g_1 . We found a significant decline in g_1 from morning to evening for the six species ($P < 0.05$, Table 2). g_1 was on average 2.5 times higher in the early morning than in the late afternoon; however, the magnitude of the decline differed between species (Fig. 9). Unlike g_1 , g_0 did not differ by the time-of-day for the six species ($P = 0.432$).

Canopy level transpiration simulations

To assess the impact of data collection methodology on model performance, we compared estimates of mean daytime E for the six species, three methods, and sap flux benchmark (when available, Fig. 10). We assumed a constant flux of E for each 15-min interval and averaged E for each 12-h diurnal period. For five of the six species, the survey data produce significantly higher ($P < 0.001$) estimates of E than for the response curve data (*B. utile* = 26.0%, *C. insignis* = 87.1%, *Guatteria dumetorum* = 124.9%, *Terminalia amazonia* = 107.4%, and *Vochysia ferruginea* = 44.3% increase). In *M. borealis*, there was no significant difference between E as estimated from curve-derived values, and E as estimated from survey-derived values ($P = 0.152$), even though in *M. borealis* the g_1 value estimated from response curves was nearly half that of the g_1 value estimated from survey measurements (Fig. 6). However, g_0 values for *M. borealis* were especially low with no significant difference between curve and survey-based estimates (Fig. S4), and *M. borealis* has a saturating irradiance, which was 50% higher than the other five species in this study Rogers *et al.* (2022).

We also found no significant differences between the survey approaches for any of the six species. In all four species for which we have a benchmark, the benchmark and survey estimates showed strong correspondence with estimates being statistically indistinguishable ($P > 0.05$).

Finally, we examined the impact of leaf phenological stage distribution assumptions on the modeling of canopy E (Fig. S8).

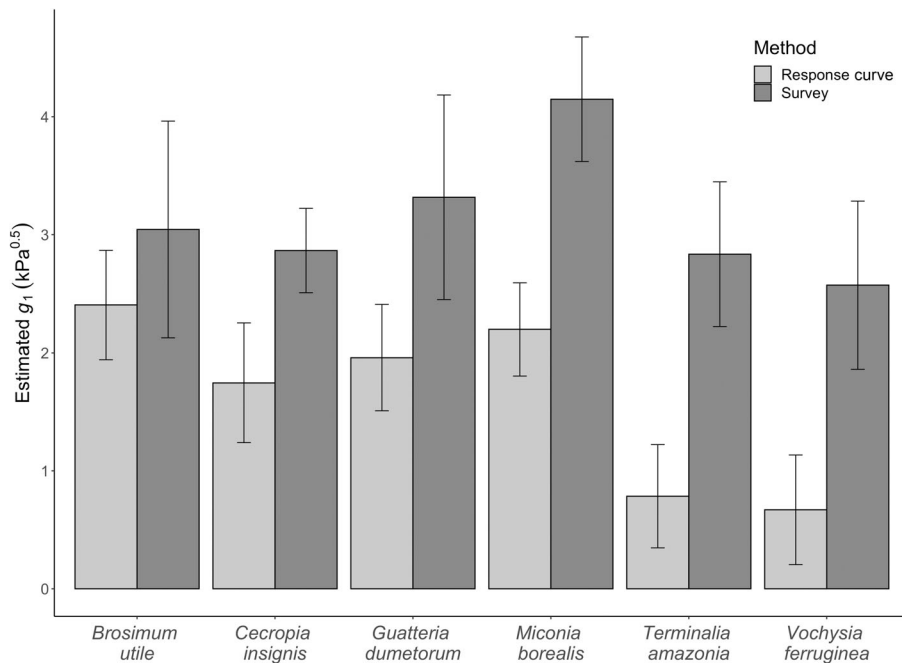


Fig. 6 Fitted values of stomatal slope (g_1) by species from the response and survey methods. *t*-Tests indicate that for all species other than *Brosimum utile* g_1 from response curves is significantly lower than g_1 estimated from the survey data ($P < 0.001$). Error bars represent ± 2 SE of the mean.

For this analysis, we reran the model prescribing different distributions of leaf phenology, including even (33.3% young, 33.3% mature, and 33.3% old), all-young, all-mature, and all-old. Interestingly, we found no significant differences in predicted daily canopy transpiration between the even phenology distribution, the ‘natural’ (15% young, 80% mature, 5% old) phenology distribution, or the all-mature phenology distribution for any species when using any of the three models of stomatal parameters. However, when modeled using a single phenological stage, we see strong variation in estimates of daily E (Fig. S8) with daily estimates of E varying by up to 150% in some species.

Discussion

A key step toward reducing ESM uncertainty is to account for the abiotic and biotic effects on the stomatal parameters g_0 and g_1 . In this study, we demonstrate that *ex situ* stomatal response curves and *in situ* survey style measurements produce statistically different estimations of stomatal parameters in tropical broadleaf evergreen forests (Fig. 6). These differences in parameterization resulted in large (between 26% and 125%) differences in simulated fluxes of water (Fig. 10). Furthermore, we found that leaf phenology plays a role in regulating stomatal traits; however, this role was not consistent across species (Figs 8, S4), was not observed consistently using the different measurement approaches (Fig. 6), and, for a given methodology, did not drive variation in modeled E (Fig. S8). We also observed a consistent decline in g_1 during the photoperiod (Fig. 9), with g_1 declining by an average of 250%. When these results are taken together and used to model forest function, we found that models using stomatal parameters derived from *ex situ* response curves significantly underestimated canopy level E both at instantaneous time scales (Fig. S3) and across a full dry season (Fig. 7), and that

while leaf traits do vary among leaf phenological stage, models, which only include mature vegetation, perform similarly to those that explicitly simulate three leaf stages (Fig. S8).

Derivation of stomatal model parameters is highly sensitive to the method of data collection

One of the clearest observations from this study is the significant difference in fitted values of g_1 between response curves and survey style measurements. In five of the six species studied, g_1 was significantly lower (50% reduction) for response curves than for survey measurements (Fig. 6). We explore several possible mechanistic explanations for the observed difference in g_1 estimates.

All response curves were measured on excised branch segments. While previous work on tropical tree species has shown that excision does not impair photosynthetic function (Verryckt *et al.*, 2020), stomata will be affected more acutely by hydraulic damage than chloroplasts if branches are not allowed to sufficiently rehydrate before measurement (Wolf *et al.*, 2016; Lawson & Viallet-Chabrand, 2019). This decline in g_s , without a commensurate decline in A (Davidson *et al.*, 2022), may result in a decrease in estimated g_1 . An excision effect was observed previously in plants collected from the same site as this study, where levels of A and g_s diminished from pre-excision values within 60 min of branch removal (Santiago & Mulkey, 2003). Here, the researchers attributed excision-induced embolism as the likely mechanism underlying their result. Missik *et al.* (2021) found that immediately following excision, levels of g_s were reduced by up to 62% in woody deciduous trees, again attributing this decline to embolism. However, in both studies, branches were cut during the daytime when transpiration fluxes are higher, and the risk of embolism is much greater (Sperry, 2013). Furthermore, Santiago & Mulkey (2003) limited their experiment to just

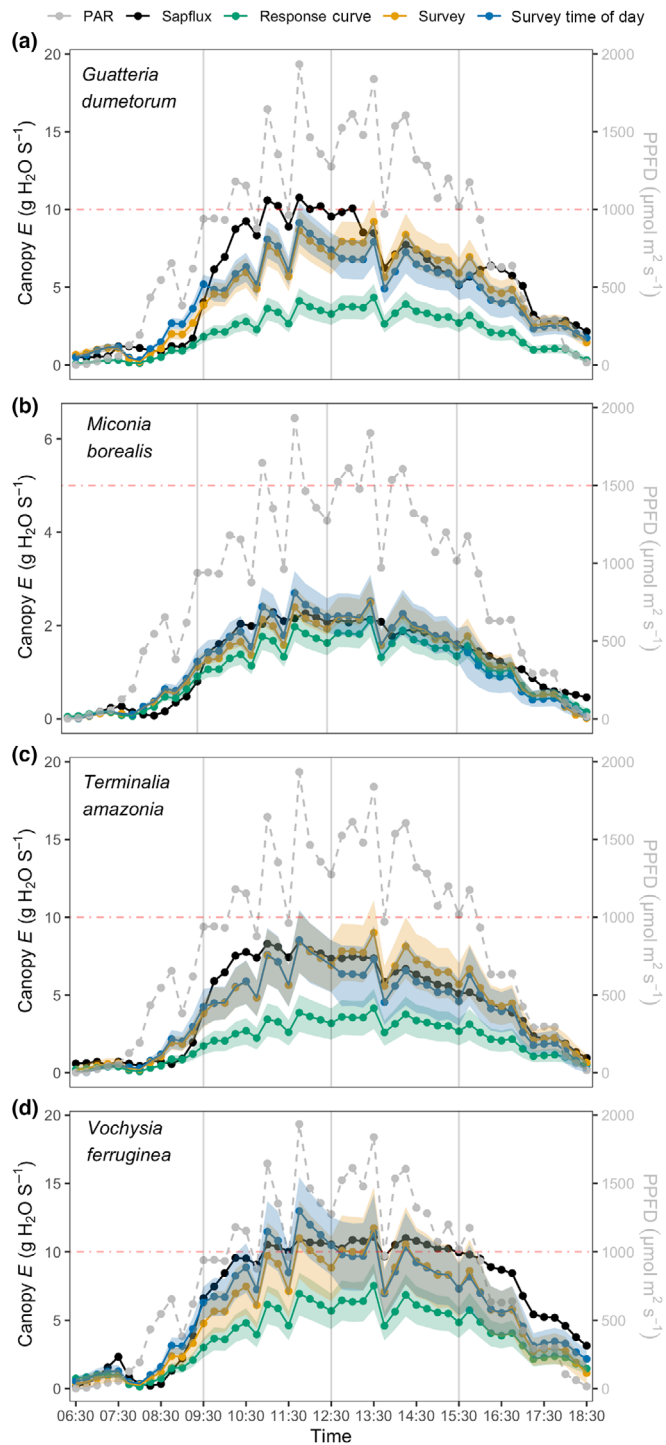


Fig. 7 Simulated canopy-scale transpiration (E , $\text{g H}_2\text{O s}^{-1}$) at 15 min time points. Data presented are for (a) *Guatteria dumetorum*, (b) *Miconia borealis*, (c) *Terminalia amazonia*, and (d) *Vochysia ferruginea* observed on 20 February 2020. Black points and line represent the sapflux benchmark, green points and line represent response curve-derived simulation, gold points and line represent survey-derived simulation, and blue points and line represent survey-derived simulation with stomatal slope (g_1) changing based on time-of-day. Shading around the simulated data represents error propagated into the simulation by using $g_1 \pm 1$ SE of the estimated value. Grey dashed line represents the solar profile (PPFD), vertical grey lines show the transition between g_1 values for the survey time-of-day model, and horizontal red line shows the level of saturating irradiance for each species.

60 minutes, which may not be sufficient time for branches to rehydrate and acclimate to a new leaf-level environment. Other studies (e.g. Meng & Arp, 1993; Miyazawa *et al.*, 2011) have found mixed, and sometimes contrasting effects of excision on gas exchange measurements.

A more relevant comparison may be drawn between this study and Davidson *et al.* (2022) who, in a comparison of cut and uncut branch segments, demonstrated that in a woody deciduous species when excision is carried out predawn, stomatal behavior is not significantly altered in leaves measured within 8 h of excision. We observed no significant difference in g_0 or g_1 estimated from curves conducted in the morning (07:00–12:00 h) and the afternoon (12:01–18:00 h) local time (Fig. S9) suggesting that excision stress did not alter stomatal function over the course of measurements. In addition, longer duration response curves were correlated with higher estimates of g_1 (Fig. S10), again suggesting that a stress response is not accumulating during measurement.

It is also possible that the direction of the response curve (increasing irradiance vs decreasing irradiance), combined with an asymmetrical response of stomata to long-term changes in irradiance (Lawson & Blatt, 2014), may have led to the negative bias observed for g_1 . To test this, we collected response curves in both directions on a similar set of tropical species (Fig. S11); however, we did not observe any evidence for a negative bias associated with curves in which irradiance is reduced.

There could also be error associated with the survey measurements. Accurate survey assessment of the $A : g_s$ relationship relies upon the assumption that levels of A and g_s are at a steady state (Hölttä *et al.*, 2017), and are acclimated to the environment surrounding the leaf, however errors when selecting an appropriate level of PPFD, VPD_{leaf} or C_a will cause alteration of the leaf-level environment. Taking irradiance as an example; if an incorrect level of irradiance is chosen, the level of assimilation will change rapidly in response to the new irradiance; however, the stomatal response will lag, which will alter the estimate of g_1 . Stomata are known to react more slowly to increases in irradiance than decreases in irradiance (Lawson & Vialet-Chabrand, 2019). This means that if, on average, we misestimated irradiance in the same proportion (equal under and over-estimation), we would expect a slightly lower WUE (higher g_1) for survey data, which is consistent with our findings (Fig. 6). This issue of improperly estimated irradiance is not insignificant, as irradiance can fluctuate dramatically, particularly under cloudy conditions (Fig. 7), which may lead to errors matching the natural environment to the leaf chamber conditions.

A final factor to consider is the leaf-to-leaf variability implicit in each measurement type, with survey measurements consisting of roughly 10 times the number of individual leaves as response curves (Fig. S2). Survey measurements showed a slightly poorer performance and a significantly higher variance, in an internal model calibration than curve-derived measurements (Fig. S12; Tables S1, S2). This may be due to the larger leaf-to-leaf variability captured using the survey method, or it could be due to unstable ambient conditions at the time of measurement which can create noise in survey data (Figs S2b, S13c,d). When the two models were validated using an external dataset comprised of c .

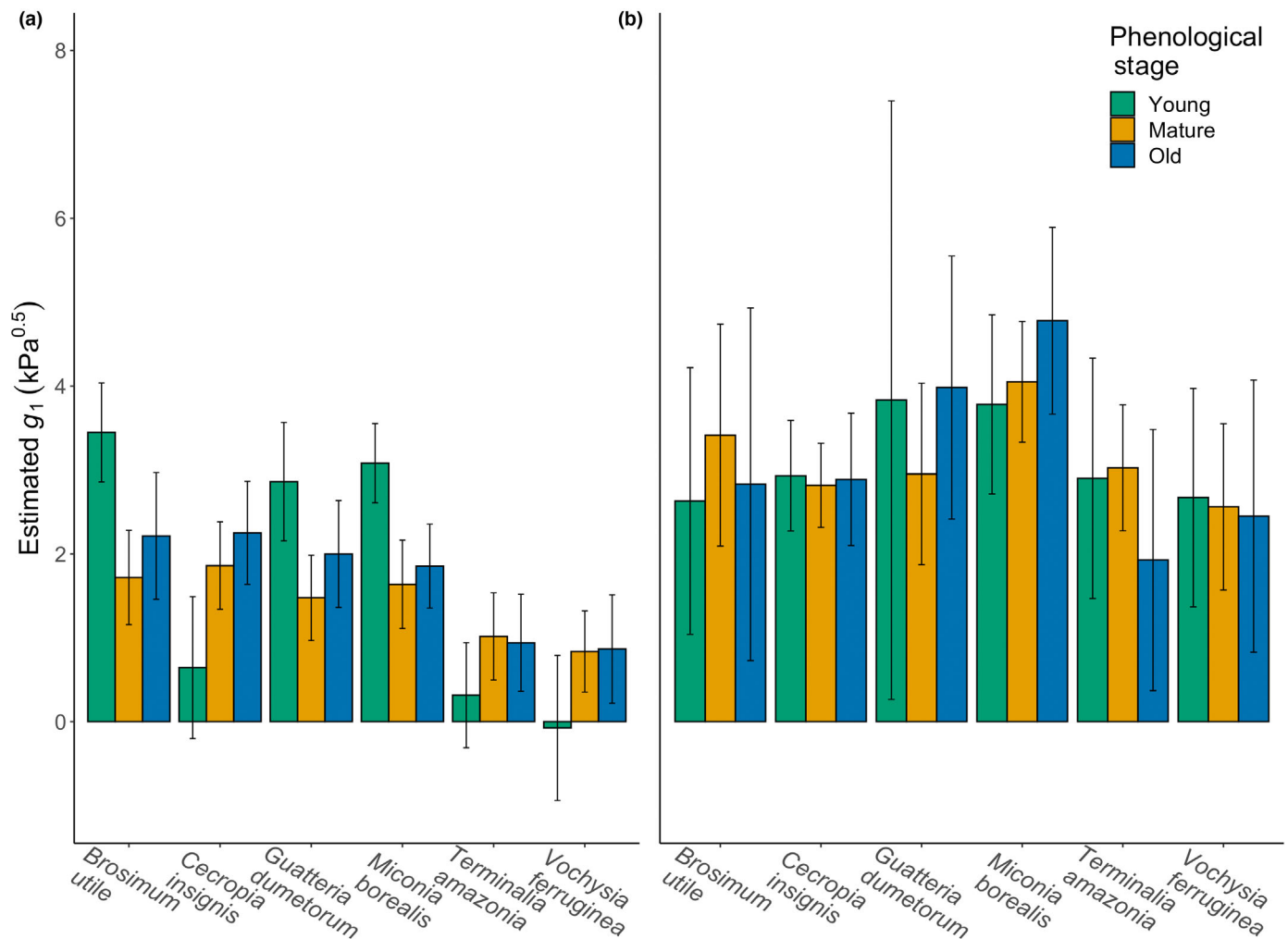


Fig. 8 Fitted values of stomatal slope (g_1) estimated using data from the two measurement methods. Estimates are from (a) response curve data, and (b) survey data. Analysis of Variance and *post hoc* Tukey tests indicates that data in (a) are significant to the species and phenological stage levels, while data in (b) were only significant at the species level. Error bars represent ± 2 SE of the mean.

120 new individual leaf estimates per species, both models had similar residual variation, while the response curve model exhibited a clear bias, underestimating levels of g_s (Fig. 5).

Clearly, both methods have benefits and drawbacks, and neither is free from error. Survey style measurements can integrate the diurnal dynamics of stomatal response, which may be an appealing feature for those who model stomatal response to a range of multivariate environmental conditions. Response curves capture stomatal response at truly stabilized conditions, which, while stability of environment rarely occurs in nature, is useful for developing generalizable parameter estimates, which can be used in ESMs.

The effect of leaf phenology and traits on g_0 and g_1

Previous work documenting phenological changes in leaf properties in wet evergreen tropical forest found a strong effect of leaf phenology on V_{cmax} (Kitajima *et al.*, 1997; Wu *et al.*, 2017). This change in V_{cmax} leads to a change in potential A , and an assumed commensurate change in the potential g_s , driven by changes in

leaf-level metabolism (Tobin & Rogers, 1992; Wingler *et al.*, 2004). However, if the relationship between A and g_s is not coordinated across leaf development, g_1 will vary between leaf phenological stages. Theoretically, a phenology-related increase in g_1 , as observed in *C. insignis* (Fig. 8a), may be adaptive as a means of maximizing the photosynthetic efficiency of older vegetation. If V_{cmax} declines in older vegetation, as we observe in this study (Fig. S7), we may also expect an increase in g_1 as a higher level of intercellular carbon (C_i) is required for the same rate of A . However, in this study, we did not find evidence across all species for a consistent effect of leaf phenological stage or relative leaf age on g_1 or g_0 (Fig. 8). Here, we explore two possible explanations for the lack of an effect observed in our study.

In the USO model, the relationship between A and g_s is the chief control on the g_1 parameter. Coordination between A and g_s means that for a given level of A , there is a given level of g_s , and thus a given level of C_i . Conversely, if A and g_s lack coordination, at a given level of A , g_s , and thus C_i , can vary. Therefore, tight coordination between A and g_s will result in leaves maintaining a fixed ratio of $C_i : C_a$ across changes in photosynthetic capacity

Table 2 Fixed effects components from the mixed effects models tested.

Model	Effect	Numerator df	Denominator df	F-value	P-value
Response curve	$g_0 \sim \text{species}$	6	607	94.30	<0.0001
	$g_0 \sim \text{stage}$	2	607	10.30	<0.001
	$g_0 \sim \text{stage} : \text{species}$	10	607	3.13	<0.001
	$g_1 \sim \text{species}$	6	607	110.67	<0.001
	$g_1 \sim \text{stage}$	2	607	4.73	0.009
	$g_1 \sim \text{stage} : \text{species}$	10	607	5.31	<0.001
Survey	$g_0 \sim \text{species}$	6	629	630.08	<0.001
	$g_0 \sim \text{stage}$	2	629	25.61	<0.001
	$g_0 \sim \text{stage} : \text{species}$	10	629	9.10	<0.001
	$g_1 \sim \text{species}$	6	629	118.21	<0.001
	$g_1 \sim \text{stage}$	2	629	0.08	0.922
	$g_1 \sim \text{stage} : \text{species}$	10	629	0.50	0.889
Survey + time-of-day	$g_0 \sim \text{species}$	6	623	764.05	<0.001
	$g_0 \sim \text{stage}$	2	623	31.06	<0.001
	$g_0 \sim \text{stage} : \text{species}$	10	623	11.04	<0.001
	$g_1 \sim \text{species}$	6	623	143.35	<0.001
	$g_1 \sim \text{time}$	3	623	124.29	<0.001
	$g_1 \sim \text{time} : \text{species}$	18	623	8.11	<0.001

A full description of each model, and the random effects components are provided in Notes S1.

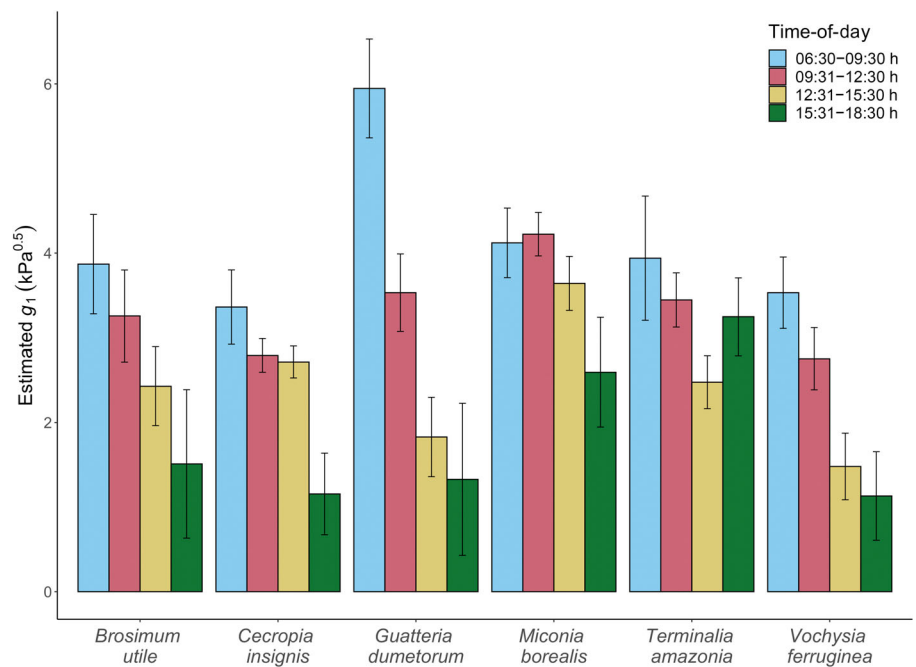


Fig. 9 Trends in fitted values of stomatal slope (g_1) by time-of-day and species. g_1 decreases significantly with increasing time-of-day for all six species investigated. *Brosimum utile*, *Cecropia insignis*, *Guatteria dumetorum*, and *Vochysia ferruginea*, all exhibit a very strong and consistent decline in g_1 , whereas *Miconia borealis* and *Terminalia amazonia* exhibit a more moderate decline. Error bars represent ± 2 SE of the mean.

(Wong *et al.*, 1979, 1985; McDowell *et al.*, 2006). We did not find significant differences in $C_i : C_a$ across any of the phenological stages across species (Fig. S14), suggesting that although V_{cmax} may shift with leaf phenology (Fig. S7a), g_s will change in proportion to supply and maintain a stable level of intercellular CO_2 (Long & Hällgren, 1993). This coordination in V_{cmax} and g_{smax} (g_s at saturating irradiance) is indicative of stable WUE or g_1 across phenological stages (Fig. 8). However, this does not suggest a lack of optimization of carbon capture through ontogeny. Even though the ratio of A and g_s does not change with leaf phenology, V_{cmax} changes with leaf phenology (Fig. S7a).

Time-of-day effect on g_1

While g_1 is often thought to be fixed over daily to seasonal time-scales (Medlyn *et al.*, 2011), others suggest that at the leaf level, g_1 may vary over shorter, diurnal time scales (Katul *et al.*, 2010). Daytime adjustments in g_1 may be driven by rapidly changing external stimuli such as irradiance (Way & Percy, 2012; Campany *et al.*, 2016), or VPD and C_a (Katul *et al.*, 2009), to which individual leaves may alter their stomatal response in order to maximize assimilation, or minimize water loss. Supply and demand dynamics may also effect stomatal behavior, with a

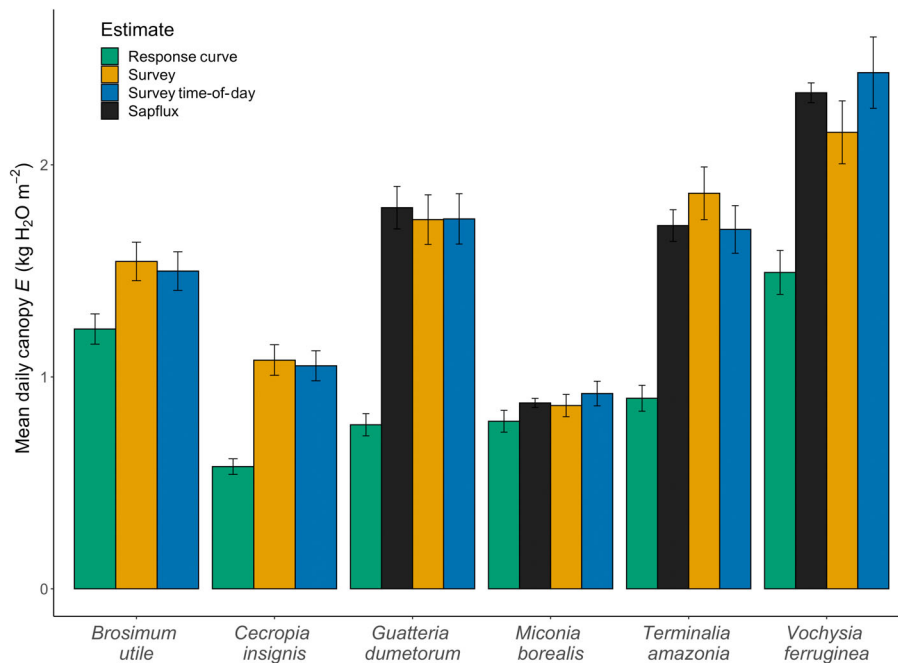


Fig. 10 Comparison of estimated mean total daily canopy transpiration (E , kg H₂O m⁻² ground area) using the three models (response curve, survey, and survey + time-of-day). Sapflux benchmark values are presented for four of the six species in this study. Mean values are the average integrated total of E over the 42 diurnal (05:30–18:30 h) periods of complete sapflux coverage. Error bars represent ± 2 SE of the mean.

reduction in the water supply to the substomatal cavity (Bonan *et al.*, 2014), leading to a more conservative response. Here, we observed declining g_1 over the diurnal periods for all six species (Fig. 9).

A decreased supply of water to the leaf late in the day (Venturas *et al.*, 2017) may be the most likely explanation for the observed decrease in g_1 . In this case, lower g_s at the same level of stomatal index (a term representing A at a combination of leaf-level environmental conditions) would result in a decrease in the fitted value of g_1 (Fig. S15). These findings are consistent with other studies of stomatal response (Manzoni *et al.*, 2011), which suggest that WUE responds to short-term changes in the supply of water. Longer term adjustments in WUE in response to seasonal or yearly drought do not appear to be occurring at this site (Wu *et al.*, 2019b).

The finding that g_1 declines throughout the day is also consistent with models of stomatal optimality, which apply a penalty on stomatal opening, either in the form of vascular damage (Wolf *et al.*, 2016; Sperry *et al.*, 2017; Anderegg *et al.*, 2018) or in non-stomatal limitations on A (Hölttä *et al.*, 2017; Dewar *et al.*, 2018; Kennedy *et al.*, 2019). Many of these models apply a function where stomata reduce their aperture in response to Ψ_{leaf} (Klein, 2014). To investigate whether Ψ_{leaf} can help explain the diurnal dynamics of g_1 , we implemented the optimality model described in Anderegg *et al.* (2018). This model applies a reduction in estimated g_s , which is proportional to the assumed decline in stem xylem conductivity with increasing Ψ_{leaf} (see also Notes S3; Table S4). However, we found that the Ψ_{leaf} penalty from Anderegg *et al.* (2018) poorly explained observed patterns of g_s (Fig. S16). Examination of stomatal model residuals vs measured Ψ_{leaf} (Fig. S6) demonstrates that Ψ_{leaf} as an explanatory factor alone, is not capable of explaining the variation in g_1 observed, consistent with previous observations (Wu *et al.*, 2019b). As an alternative to Ψ_{leaf} based models,

many ESMs use a β factor, dictated by soil moisture, to downregulate V_{cmax} and g_s . Recently, Li *et al.* (2022) tested the applicability of a β factor at the same site in this study and found that, like Anderegg *et al.* (2018), it overpenalized drought-related loss of productivity. Several other hydraulic parameters such as hydraulic capacitance and leaf hydraulic conductance may be more pertinent and may play a larger role in stomatal regulation; however, we lack those data in this current study.

The low morning WUE observed across all species may be the result of circadian resonance (Green *et al.*, 2002), whereby sunrise anticipation linked to a plant's endogenous rhythm may prime stomata to achieve their largest opening early in the day. This behavior, in systems with a fixed photoperiod, is thought to be adaptive as a means of maximizing carbon assimilation (Resco de Dios *et al.*, 2016). Higher than optimal morning g_s would lead to elevated estimates of g_1 , which is consistent with previous findings that suggest circadian regulation fails to help to optimize diurnal variations in stomatal conductance (Resco de Dios *et al.*, 2020).

The failure of a time-of-day effect to significantly improve predictions of g_s (Fig. 5) suggests that while an overall pattern of declining g_1 is expected, the magnitude of the decline each day is the by-product of abiotic processes that we may not have fully captured in this study, such as dynamics in the soil–plant–atmosphere continuum (Zhang *et al.*, 2018), or an effect of ABA on regulating stomata (McAdam & Brodribb, 2015). Without these data, and a more detailed understanding of the response of stomata to small changes in VPD (Buckley, 2016), it may not be possible to model diurnal fluctuations in WUE. Thus, we recommend future research explore diurnal shifts in g_1 in greater detail, as an understanding of the mechanisms behind these dynamics has the potential to significantly advance our model representation of canopy E .

Impact of measurement method on models of canopy function

Our simulations of canopy E revealed that using parameters derived from response curves leads to a systematically underestimated (26–125%) diurnal flux (Figs 7, 10), consistent with our external model validation (Figs 5, S3). This underestimation is in part attributable to lower g_1 values from response curves (Fig. 6) which limit daytime E , due to the assumption that at an irradiance level greater than saturating, $g_s = g_{smax}$.

All three models underestimate the level of E at low irradiance as the simulations assume that any time irradiance is below the light compensation point, $g_s = g_0$. However, this assumption may be flawed due to the combination of cuticular conductance and stomatal leakage (Machado *et al.*, 2021), measurement artifacts (Duursma *et al.*, 2019), or unaccounted for transpiration from stored crown water supplies (Meinzer *et al.*, 2003). The integrated diurnal flux of water (Fig. 10) also reveals a large impact of parameterization, with the survey method producing species level values of E between 9% and 77% higher than model output using response curve-derived parameters, underscoring the impact that g_1 can have on model estimation of ecosystem function (Dietze *et al.*, 2014) and reinforcing the need for careful choices with regard to the method used to estimate g_1 .

Finally, in our assessment of the impact of selected phenological distribution on simulations of canopy E (Fig. S8), we observed no significant difference in daily E between models run using a natural leaf distribution an even phenological distribution or an all-mature distribution. Previous work in the Brazilian Amazon has suggested that appropriate estimation of leaf phenological distribution is essential for accurate estimation of gross primary productivity (GPP) and canopy A_{net} (Wu *et al.*, 2016, 2017). The fact that our models of E are not sensitive to leaf age distribution may be due in part to the limited role leaf phenology plays in stomatal traits (Fig. 8), with the majority of between phenological stage variation being modeled as variation in V_{cmax} (Fig. S7; Wu *et al.*, 2019a). While V_{cmax} plays a role in determining g_s and therefore E , variation in the g_1 and g_0 parameters would be expected to manifest in larger variation in E (Rogers *et al.*, 2017). Our findings underscore the need to closely consider the method used, and assumptions implicit to that method, when parameterizing generic PFTs, or when applying trait-based approaches to ESMs (Van Bodegom *et al.*, 2012).

Acknowledgements

We would like to thank the staff of the STRI for assistance with field logistics and support during data collection, particularly Edwin Andrades for his skillful crane driving. This work was supported by the Next-Generation Ecosystem Experiments (NGEE) – Tropics project, which is funded by the Biological and Environmental Research (BER) Program within the US Department of Energy's (DOE) Office of Science and through DOE contract no. DE-SC0012704 to Brookhaven National Laboratory. BTW was supported by the National Institute of Food and Agriculture,

US Department of Agriculture, McIntire Stennis project under LAB94493.

Author contributions

KJD, JL, AR, SJW and SPS conceived the study. KJD, JL, AR, KSE and SPS contributed to the leaf-level data collection and quality checking. NM, ALP, BTW and AZ contributed to the sap flux data. KJD, JL, AR, QL, ALP, BTW and SPS analyzed the data. KJD drafted the manuscript, and all authors contributed to the final version.

Competing interests

None declared.

ORCID

Kenneth J. Davidson  <https://orcid.org/0000-0001-5745-9689>

Kim S. Ely  <https://orcid.org/0000-0002-3915-001X>

Julien Lamour  <https://orcid.org/0000-0002-4410-507X>

Qianyu Li  <https://orcid.org/0000-0002-0627-039X>

Nate G. McDowell  <https://orcid.org/0000-0002-2178-2254>

Alexandria L. Pivovarovoff  <https://orcid.org/0000-0002-3104-1900>

Alistair Rogers  <https://orcid.org/0000-0001-9262-7430>

Shawn P. Serbin  <https://orcid.org/0000-0003-4136-8971>

Brett T. Wolfe  <https://orcid.org/0000-0001-7535-045X>

S. Joseph Wright  <https://orcid.org/0000-0003-4260-5676>

Alfonso Zambrano  <https://orcid.org/0000-0001-5442-5897>

Data availability

Gas exchange data that support the findings of this study are publicly available in: Lamour *et al.* (2021b) and Rogers *et al.* (2022). Leaf trait data that support the findings of this study are publicly available in: Lamour *et al.* (2022a). Spectroscopic data that support the findings of this study are publicly available in: Lamour *et al.* (2021a). Sap flux data that support the findings of this study are publicly available in: Pivovarovoff *et al.* (2020).

References

- Ainsworth EA, Rogers A. 2007. The response of photosynthesis and stomatal conductance to rising [CO₂]: mechanisms and environmental interactions: photosynthesis and stomatal conductance responses to rising [CO₂]. *Plant, Cell & Environment* 30: 258–270.
- Anderegg WRL, Wolf A, Arango-Velez A, Choat B, Chmura DJ, Jansen S, Kolb T, Li S, Meinzer F, Pita P *et al.* 2017. Plant water potential improves prediction of empirical stomatal models. *PLoS ONE* 12: e0185481.
- Anderegg WRL, Wolf A, Arango-Velez A, Choat B, Chmura DJ, Jansen S, Kolb T, Li S, Meinzer FC, Pita P *et al.* 2018. Woody plants optimise stomatal behaviour relative to hydraulic risk. *Ecology Letters* 21: 968–977.
- Ball TJ, Woodrow IE, Berry JA. 1987. A model predicting stomatal conductance and its contribution to the control of photosynthesis under different environmental conditions. In: Biggins J, ed. *Progress in photosynthesis research*. Dordrecht, the Netherlands: Springer, 221–224.

- Bauerle WL, Daniels AB, Barnard DM. 2014. Carbon and water flux responses to physiology by environment interactions: a sensitivity analysis of variation in climate on photosynthetic and stomatal parameters. *Climate Dynamics* 42: 2539–2554.
- Béland M, Baldocchi DD. 2021. Vertical structure heterogeneity in broadleaf forests: effects on light interception and canopy photosynthesis. *Agricultural and Forest Meteorology* 307: 108525.
- Bernacchi CJ, Leakey ADB, Heady LE, Morgan PB, Dohleman FG, Mcgrath JM, Gillespie KM, Wittig VE, Rogers A, Long SP *et al.* 2006. Hourly and seasonal variation in photosynthesis and stomatal conductance of soybean grown at future CO₂ and ozone concentrations for 3 yr under fully open-air field conditions. *Plant, Cell & Environment* 29: 2077–2090.
- Bernacchi CJ, Singsaas EL, Pimentel C, Portis AR Jr, Long SP. 2001. Improved temperature response functions for models of Rubisco-limited photosynthesis: *in vivo* Rubisco enzyme kinetics. *Plant, Cell & Environment* 24: 253–259.
- Bonan G. 2008. *Ecological climatology: concepts and applications*. Cambridge, UK: Cambridge University Press.
- Bonan GB, Williams M, Fisher RA, Oleson KW. 2014. Modeling stomatal conductance in the earth system: linking leaf water-use efficiency and water transport along the soil–plant–atmosphere continuum. *Geoscientific Model Development* 7: 2193–2222.
- Buckley TN. 2016. Stomatal responses to humidity: has the ‘black box’ finally been opened?: stomatal responses to humidity. *Plant, Cell & Environment* 39: 482–484.
- Buckley TN, Martorell S, Diaz-Espejo A, Tomàs M, Medrano H. 2014. Is stomatal conductance optimized over both time and space in plant crowns? A field test in grapevine (*Vitis vinifera*). *Plant, Cell & Environment* 37: 2707–2721.
- Campany CE, Tjoelker MG, von Caemmerer S, Duursma RA. 2016. Coupled response of stomatal and mesophyll conductance to light enhances photosynthesis of shade leaves under sunflecks: mesophyll conductance response to light. *Plant, Cell & Environment* 39: 2762–2773.
- Condit R, Windsor DM, Hubbell SP. 2013. *NPP tropical forest: Barro Colorado, Panama, 1969–1990, R1*. Oak Ridge, TN, USA: ORNL DAAC. doi: [10.3334/ORNLDAAC/157](https://doi.org/10.3334/ORNLDAAC/157).
- Cowan IR. 1978. Stomatal behaviour and environment. In: Preston RD, Woolhouse HW, eds. *Advances in botanical research*. London, UK: Academic Press, 117–228.
- Cowan IR, Farquhar GD. 1977. Stomatal function in relation to leaf metabolism and environment. In: Jennings D, ed. *Integration of activity in the higher plant*. Cambridge, UK: Cambridge University Press, 471–505.
- Damour G, Simonneau T, Cochard H, Urban L. 2010. An overview of models of stomatal conductance at the leaf level: models of stomatal conductance. *Plant, Cell & Environment* 39: 1419–1438.
- Davidson KJ, Lamour J, Serbin SP, Rogers A. 2022. Late day measurement of excised branches results in uncertainty in the estimation of two stomatal parameters derived from response curves in *Populus deltoides* Bartr. × *Populus nigra* L. *Tree Physiology* 42: 1377–1395.
- De Weirdt M, Verbeeck H, Maignan F, Peylin P, Poulter B, Bonal D, Ciais P, Steppe K. 2012. Seasonal leaf dynamics for tropical evergreen forests in a process-based global ecosystem model. *Geoscientific Model Development* 5: 1091–1108.
- Dewar R, Mauranen A, Mäkelä A, Hölttä T, Medlyn B, Vesala T. 2018. New insights into the covariation of stomatal, mesophyll and hydraulic conductances from optimization models incorporating nonstomatal limitations to photosynthesis. *New Phytologist* 217: 571–585.
- Dietze MC, Serbin SP, Davidson C, Desai AR, Feng X, Kelly R, Kooper R, LeBauer D, Mantooth J, McHenry K *et al.* 2014. A quantitative assessment of a terrestrial biosphere model’s data needs across North American biomes: PEcAn/ED model-data uncertainty analysis. *Journal of Geophysical Research: Biogeosciences* 119: 286–300.
- Domingues TF, Martinelli LA, Ehleringer JR. 2014. Seasonal patterns of leaf-level photosynthetic gas exchange in an eastern Amazonian rain forest. *Plant Ecology & Diversity* 7: 189–203.
- Duursma RA, Blackman CJ, López R, Martin-StPaul NK, Cochard H, Medlyn BE. 2019. On the minimum leaf conductance: its role in models of plant water use, and ecological and environmental controls. *New Phytologist* 221: 693–705.
- Farquhar GD, Wong SC. 1984. An empirical model of stomatal conductance. *Functional Plant Biology* 11: 191–210.
- Franklin O. 2007. Optimal nitrogen allocation controls tree responses to elevated CO₂. *New Phytologist* 174: 811–822.
- Franks PJ, Lombardozzi L, Bonan GB, Berry JA, Holbrook NM, Herold N, Oleson KW. 2018. Comparing optimal and empirical stomatal conductance models for application in earth system models. *Global Change Biology* 24: 5708–5723.
- Granier A. 1987. Evaluation of transpiration in a Douglas-fir stand by means of sap flow measurements. *Tree Physiology* 3: 309–320.
- Green RM, Tingay S, Wang Z-Y, Tobin EM. 2002. Circadian rhythms confer a higher level of fitness to Arabidopsis plants. *Plant Physiology* 129: 576–584.
- Hérault A, Lin Y-S, Bourne A, Medlyn BE, Ellsworth DS. 2013. Optimal stomatal conductance in relation to photosynthesis in climatically contrasting *Eucalyptus* species under drought: stomatal responses of eucalyptus under drought. *Plant, Cell & Environment* 36: 262–274.
- Hetherington AM, Woodward FI. 2003. The role of stomata in sensing and driving environmental change. *Nature* 424: 901–908.
- Hölttä T, Lintunen A, Chan T, Mäkelä A, Nikinmaa E. 2017. A steady-state stomatal model of balanced leaf gas exchange, hydraulics and maximal source–sink flux. *Tree Physiology* 37: 851–868.
- Jefferson JL, Maxwell RM, Constantine PG. 2017. Exploring the sensitivity of photosynthesis and stomatal resistance parameters in a land surface model. *Journal of Hydrometeorology* 18: 879–915.
- Katul G, Manzoni S, Palmroth S, Oren R. 2010. A stomatal optimization theory to describe the effects of atmospheric CO₂ on leaf photosynthesis and transpiration. *Annals of Botany* 105: 431–442.
- Katul GG, Palmroth S, Oren R. 2009. Leaf stomatal responses to vapour pressure deficit under current and CO₂-enriched atmosphere explained by the economics of gas exchange. *Plant, Cell & Environment* 32: 968–979.
- Kennedy D, Swenson S, Oleson KW, Lawrence DM, Fisher R, Lola da Costa AC, Gentine P. 2019. Implementing plant hydraulics in the community land model, v.5. *Journal of Advances in Modeling Earth Systems* 11: 485–513.
- Kitajima K, Mulkey SS, Samaniego M, Joseph WS. 2002. Decline of photosynthetic capacity with leaf age and position in two tropical pioneer tree species. *American Journal of Botany* 89: 1925–1932.
- Kitajima K, Mulkey SS, Wright SJ. 1997. Decline of photosynthetic capacity with leaf age in relation to leaf longevities for five tropical canopy tree species. *American Journal of Botany* 84: 702–708.
- Klein T. 2014. The variability of stomatal sensitivity to leaf water potential across tree species indicates a continuum between isohydric and anisohydric behaviours. *Functional Ecology* 28: 1313–1320.
- Knapp AK. 1993. Gas exchange dynamics in C³ and C⁴ grasses: consequence of differences in stomatal conductance. *Ecology* 74: 113–123.
- Lamour J, Davidson K, Ely K, Anderson J, Rogers A, Serbin S. 2021a. *Leaf spectral reflectance and transmittance, San Lorenzo, Panama, 2020. 1.0. NGEETropics Data Collection* (dataset). doi: [10.15486/ngt/1781003](https://doi.org/10.15486/ngt/1781003).
- Lamour J, Davidson K, Ely K, Anderson J, Rogers A, Serbin S. 2022a. *Leaf structural and chemical traits, and BNL field campaign sample details, San Lorenzo, Panama, 2020. 1.0. NGEETropics Data Collection* (dataset). doi: [10.15486/ngt/1783737](https://doi.org/10.15486/ngt/1783737).
- Lamour J, Davidson KJ, Ely KS, Anderson J, Serbin SP, Rogers A. 2021b. *Leaf gas exchange and fitted parameters, San Lorenzo, Panama, 2020. 1.0. NGEETropics Data Collection* (dataset). doi: [10.15486/ngt/1781004](https://doi.org/10.15486/ngt/1781004).
- Lamour J, Davidson KJ, Ely KS, Anderson JA, Rogers A, Wu J, Serbin SP. 2021c. Rapid estimation of photosynthetic leaf traits of tropical plants in diverse environmental conditions using reflectance spectroscopy. *PLoS ONE* 16: e0258791.
- Lamour J, Davidson KJ, Ely KS, Le Moguédec G, Leakey ADB, Li Q, Serbin SP, Rogers A. 2022b. An improved representation of the relationship between photosynthesis and stomatal conductance leads to more stable estimation of conductance parameters and improves the goodness-of-fit across diverse data sets. *Global Change Biology* 28: 3537–3556.
- Lamour J, Davidson KJ, Ely KS, Li Q, Serbin SP, Rogers A. 2022c. New calculations for photosynthesis measurement systems: what’s the impact for physiologists and modelers? *New Phytologist* 233: 592–598.

- Lamour J, Serbin SP. 2021. *LeafGasExchange*. doi: [10.5281/zenodo.4545818](https://doi.org/10.5281/zenodo.4545818).
- Lawson T, Blatt MR. 2014. Stomatal size, speed, and responsiveness impact on photosynthesis and water use efficiency. *Plant Physiology* **164**: 1556–1570.
- Lawson T, Vialat-Chabrand S. 2019. Speedy stomata, photosynthesis and plant water use efficiency. *New Phytologist* **221**: 93–98.
- Leach JE, Woodhead T, Day W. 1982. Bias in pressure chamber measurements of leaf water potential. *Agricultural Meteorology* **27**: 257–263.
- Leakey ADB, Bernacchi CJ, Ort DR, Long SP. 2006. Long-term growth of soybean at elevated [CO₂] does not cause acclimation of stomatal conductance under fully open-air conditions. *Plant, Cell & Environment* **29**: 1794–1800.
- Leuning R. 1995. A critical appraisal of a combined stomatal-photosynthesis model for C³ plants. *Plant, Cell & Environment* **18**: 339–355.
- Li Q, Serbin SP, Lamour J, Davidson KJ, Ely KS, Rogers A. 2022. Implementation and evaluation of the unified stomatal optimization approach in the Functionally Assembled Terrestrial Ecosystem Simulator (FATES). *Geoscientific Model Development* **15**: 4313–4329.
- Lin Y-S, Medlyn BE, Duursma RA, Prentice IC, Wang H, Baig S, Eamus D, de Dios VR, Mitchell P, Ellsworth DS *et al.* 2015. Optimal stomatal behaviour around the world. *Nature Climate Change* **5**: 459–464.
- Long SP, Hällgren J-E. 1993. Measurement of CO₂ assimilation by plants in the field and the laboratory. In: Hall DO, Scurlock JMO, Bolhár-Nordenkamp HR, Leegood RC, Long SP, eds. *Photosynthesis and production in a changing environment: a field and laboratory manual*. Dordrecht, the Netherlands: Springer, 129–167.
- Machado R, Loram-Lourenço L, Farnese FS, Alves RDFB, Sousa LF, Silva FG, Filho SCV, Torres-Ruiz JM, Cochard H, Menezes-Silva PE. 2021. Where do leaf water leaks come from? Trade-offs underlying the variability in minimum conductance across tropical savanna species with contrasting growth strategies. *New Phytologist* **229**: 1415–1430.
- Manzoni S, Vico G, Katul G, Fay PA, Polley W, Palmroth S, Porporato A. 2011. Optimizing stomatal conductance for maximum carbon gain under water stress: a meta-analysis across plant functional types and climates: optimal leaf gas exchange under water stress. *Functional Ecology* **25**: 456–467.
- Martínez Cano I, Müller-Landau HC, Wright SJ, Bohlman SA, Pacala SW. 2019. Tropical tree height and crown allometries for the Barro Colorado Nature Monument, Panama: a comparison of alternative hierarchical models incorporating interspecific variation in relation to life history traits. *Biogeosciences* **16**: 847–862.
- McAdam SAM, Brodribb TJ. 2015. The evolution of mechanisms driving the stomatal response to vapor pressure deficit. *Plant Physiology* **167**: 833–843.
- McDowell NG, Adams HD, Bailey JD, Hess M, Kolb TE. 2006. Homeostatic maintenance of ponderosa pine gas exchange in response to stand density changes. *Ecological Applications* **16**: 1164–1182.
- Medlyn BE, Duursma RA, Eamus D, Ellsworth DS, Prentice IC, Barton CVM, Crous KY, De Angelis P, Freeman M, Wingate L. 2011. Reconciling the optimal and empirical approaches to modelling stomatal conductance. *Global Change Biology* **17**: 2134–2144.
- Meidner H, Mansfield TA. 1968. *Physiology of stomata*. London, UK: McGraw-Hill.
- Meinzer FC, Goldstein G, Andrade JL. 2001. Regulation of water flux through tropical forest canopy trees: Do universal rules apply? *Tree Physiology* **21**: 19–26.
- Meinzer FC, James SA, Goldstein G, Woodruff D. 2003. Whole-tree water transport scales with sapwood capacitance in tropical forest canopy trees: water transport scales with sapwood properties in tropical trees. *Plant, Cell & Environment* **26**: 1147–1155.
- Meng F-R, Arp PA. 1993. Net photosynthesis and stomatal conductance of red spruce twigs before and after twig detachment. *Canadian Journal of Forest Research* **23**: 716–721.
- Missik JEC, Oishi AC, Benson MC, Meretsky VJ, Phillips RP, Novick KA. 2021. Performing gas-exchange measurements on excised branches – evaluation and recommendations. *Photosynthetica* **59**: 61–73.
- Miyazawa Y, Tateishi M, Komatsu H, Kumagai T, Otsuki K. 2011. Are measurements from excised leaves suitable for modeling diurnal patterns of gas exchange of intact leaves? *Hydrological Processes* **25**: 2924–2930.
- Norman JM. 1979. Modeling the complete crop canopy. In: Barfield G, ed. *Modification of the aerial environment of crops*. St Joseph, MI, USA: American Society of Agricultural Engineers, 249–277.
- Osnas JLD, Katabuchi M, Kitajima K, Wright SJ, Reich PB, Van Bael SA, Kraft NJB, Samaniego MJ, Pacala SW, Lichstein JW. 2018. Divergent drivers of leaf trait variation within species, among species, and among functional groups. *Proceedings of the National Academy of Sciences, USA* **115**: 5480–5485.
- Paton S. 2020. *Yearly reports_San Lorenzo Crane*. Balboa Ancon, Panama: Smithsonian Tropical Research Institute. [WWW document] URL https://smithsonian.figshare.com/articles/dataset/Yearly_Reports_San_Lorenzo_Crane/11799309/2 [accessed 15 February 2021].
- Pinheiro J, Bates D, DebRoy S, Sarkar D, Heisterkamp S, Bert VW. 2020. *Package 'nlme'*. [WWW document] URL <https://cran.r-project.org/web/packages/nlme/index.html> [accessed 15 February 2021].
- Pivovarov A, McDowell N, Davies S, Detto M, Wolfe BT, Wright J, Zambrano A. 2020. *Sap flow data from San Lorenzo, Panama (PA-SLZ) from January–June 2020. 1.0. Ngee Tropics Data Collection* (dataset). doi: [10.15486/ngt/1678733](https://doi.org/10.15486/ngt/1678733).
- R Core Team. 2013. *R: a language and environment for statistical computing*. Vienna, Austria: R Foundation for Statistical Computing.
- Resco de Dios V, Anderegg WRL, Li X, Tissue DT, Bahn M, Landais D, Milcu A, Yao Y, Nolan RH, Roy J *et al.* 2020. Circadian regulation does not optimize stomatal behaviour. *Plants* **9**: 1091.
- Resco de Dios V, Loik ME, Smith R, Aspinwall MJ, Tissue DT. 2016. Genetic variation in circadian regulation of nocturnal stomatal conductance enhances carbon assimilation and growth: on the function of nocturnal stomatal conductance. *Plant, Cell & Environment* **39**: 3–11.
- Ricciuto D, Sargsyan K, Thornton P. 2018. The impact of parametric uncertainties on biogeochemistry in the E3SM land model. *Journal of Advances in Modeling Earth Systems* **10**: 297–319.
- Rodríguez-Domínguez CM, Forner A, Martorell S, Choat B, Lopez R, Peters JMR, Pfautsch S, Mayr S, Carins-Murphy MR, McAdam SAM *et al.* 2022. Leaf water potential measurements using the pressure chamber: synthetic testing of assumptions towards best practices for precision and accuracy. *Plant, Cell & Environment* **45**: 2037–2061.
- Rogers A, Allen DJ, Davey PA, Morgan PB, Ainsworth EA, Bernacchi CJ, Cornic G, Dermody O, Dohleman FG, Heaton EA *et al.* 2004. Leaf photosynthesis and carbohydrate dynamics of soybeans grown throughout their life-cycle under free-air carbon dioxide enrichment. *Plant, Cell & Environment* **27**: 449–458.
- Rogers A, Medlyn BE, Dukes JS, Bonan G, von Caemmerer S, Dietze MC, Kattge J, Leakey ADB, Mercado LM, Niinemets Ü *et al.* 2017. A roadmap for improving the representation of photosynthesis in earth system models. *New Phytologist* **213**: 22–42.
- Rogers A, Serbin SP, Ely K, Wu J, Wolfe BT, Dickman LT, Collins AD, Detto M, Grossiord C, McDowell N *et al.* 2022. *Diurnal leaf gas exchange survey, Feb2016-May2016, PA-SLZ, PA-PNM: Panama. 2. Ngee Tropics Data Collection* (dataset). doi: [10.15486/ngt/1411972](https://doi.org/10.15486/ngt/1411972).
- Santiago LS, Mulkey SS. 2003. A test of gas exchange measurements on excised canopy branches of ten tropical tree species. *Photosynthetica* **41**: 343–347.
- van Schaik CP, Terborgh JW, Wright SJ. 1993. The phenology of tropical forests: adaptive significance and consequences for primary consumers. *Annual Review of Ecology and Systematics* **24**: 353–377.
- Schlesinger WH, Jasechko S. 2014. Transpiration in the global water cycle. *Agricultural and Forest Meteorology* **189–190**: 115–117.
- Scholander PF, Hammel HT, Hemmingen EA, Bradstreet ED. 1964. Hydrostatic pressure and osmotic potential in leaves of mangroves and some other plants. *Proceedings of the National Academy of Sciences, USA* **52**: 119–125.
- Sirri NF, Libalah MB, Momo Takoudjou S, Ploton P, Medjibe V, Kamdem NG, Mofack G, Sonké B, Barbier N. 2019. Allometric models to estimate leaf area for tropical African broadleaved forests. *Geophysical Research Letters* **46**: 8985–8994.
- Speckman H. 2019. *AQUAFLUX: swift and transparent analysis of plant-level transpiration*. [WWW document] URL <https://rdr.io/github/HeatherSpeckman/AquaFlux/man/AquaFlux.html> [accessed 10 March 2021].
- Sperry JS. 2013. Cutting-edge research or cutting-edge artefact? An overdue control experiment complicates the xylem refilling story: xylem-refilling artefacts. *Plant, Cell & Environment* **36**: 1916–1918.
- Sperry JS, Venturas MD, Anderegg WRL, Mencuccini M, Mackay DS, Wang Y, Love DM. 2017. Predicting stomatal responses to the environment from the optimization of photosynthetic gain and hydraulic cost: a stomatal optimization model. *Plant, Cell & Environment* **40**: 816–830.

- Tobin AK, Rogers WJ. 1992. Metabolic interactions of organelles during leaf development. In: Tobin AK, ed. *Seminar series-society for experimental biology. Plant organelles*. Cambridge, UK: Cambridge University Press, 293–323.
- Van Bodegom PM, Douma JC, Witte JPM, Ordoñez JC, Bartholomeus RP, Aerts R. 2012. Going beyond limitations of plant functional types when predicting global ecosystem-atmosphere fluxes: exploring the merits of traits-based approaches: merits of traits-based vegetation modelling. *Global Ecology and Biogeography* 21: 625–636.
- Venturas MD, Sperry JS, Hacke UG. 2017. Plant xylem hydraulics: what we understand, current research, and future challenges: plant xylem hydraulics. *Journal of Integrative Plant Biology* 59: 356–389.
- Verryckt LT, Van Langenhove L, Ciais P, Courtois EA, Vicca S, Peñuelas J, Stahl C, Coste S, Ellsworth DS, Posada JM *et al.* 2020. Coping with branch excision when measuring leaf net photosynthetic rates in a lowland tropical forest. *Biotropica* 52: 608–615.
- Von Caemmerer S. 2013. Steady-state models of photosynthesis: steady-state models of photosynthesis. *Plant, Cell & Environment* 36: 1617–1630.
- Way DA, Pearcy RW. 2012. Sunflecks in trees and forests: from photosynthetic physiology to global change biology. *Tree Physiology* 32: 1066–1081.
- Wingler A, Marès M, Pourtau N. 2004. Spatial patterns and metabolic regulation of photosynthetic parameters during leaf senescence. *New Phytologist* 161: 781–789.
- Wolf A, Anderegg WRL, Pacala SW. 2016. Optimal stomatal behavior with competition for water and risk of hydraulic impairment. *Proceedings of the National Academy of Sciences, USA* 113: E7222–E7230.
- Wolz KJ, Wertin TM, Abordo M, Wang D, Leakey ADB. 2017. Diversity in stomatal function is integral to modelling plant carbon and water fluxes. *Nature Ecology & Evolution* 1: 1292–1298.
- Wong SC, Cowan IR, Farquhar GD. 1979. Stomatal conductance correlates with photosynthetic capacity. *Nature* 282: 424–426.
- Wong SC, Cowan IR, Farquhar GD. 1985. Leaf conductance in relation to rate of CO₂ assimilation. *Plant Physiology* 78: 821–825.
- Wu J, Albert LP, Lopes AP, Restrepo-Coupe N, Hayek M, Wiedemann KT, Guan K, Stark SC, Christoffersen B, Prohaska N *et al.* 2016. Leaf development and demography explain photosynthetic seasonality in Amazon evergreen forests. *Science* 351: 972–976.
- Wu J, Rogers A, Albert LP, Ely K, Prohaska N, Wolfe BT, Oliveira RC, Saleska SR, Serbin SP. 2019a. Leaf reflectance spectroscopy captures variation in carboxylation capacity across species, canopy environment and leaf age in lowland moist tropical forests. *New Phytologist* 224: 663–674.
- Wu J, Serbin SP, Ely KS, Wolfe BT, Dickman LT, Grossiord C, Michaletz ST, Collins AD, Detto M, McDowell NG *et al.* 2019b. The response of stomatal conductance to seasonal drought in tropical forests. *Global Change Biology* 26: 823–839.
- Wu J, Serbin SP, Xu X, Albert LP, Chen M, Meng R, Saleska SR, Rogers A. 2017. The phenology of leaf quality and its within-canopy variation is essential for accurate modeling of photosynthesis in tropical evergreen forests. *Global Change Biology* 23: 4814–4827.
- Zhang J, Jiang H, Song X, Jin J, Zhang X. 2018. The responses of plant leaf CO₂/H₂O exchange and water use efficiency to drought: a meta-analysis. *Sustainability* 10: 551.
- Zhou S-X, Medlyn B, Sabaté S, Sperlich D, Prentice IC, Whitehead D. 2014. Short-term water stress impacts on stomatal, mesophyll and biochemical limitations to photosynthesis differ consistently among tree species from contrasting climates. *Tree Physiology* 34: 1035–1046.
- Zhou S-X, Medlyn BE, Prentice IC. 2016. Long-term water stress leads to acclimation of drought sensitivity of photosynthetic capacity in xeric but not riparian *Eucalyptus* species. *Annals of Botany* 117: 133–144.
- Fig. S1** Histograms of the atmospheric vapor pressure deficit (VPD_{air}) observed during survey gas exchange measurements.
- Fig. S2** Regression of stomatal response from the two different measurement methods.
- Fig. S3** Observed vs predicted fluxes of canopy-scale transpiration (*E*) for *Guatteria dumetorum*, *Miconia borealis*, *Terminalia amazonia*, and *Vochysia ferruginea* using three different methods to derive stomatal parameters.
- Fig. S4** Stomatal intercept (*g*₀) estimates by species, phenological stage, and measurement method.
- Fig. S5** Relationships between estimated stomatal and leaf functional traits.
- Fig. S6** Relationship between leaf water potential (Ψ_{leaf}) and model residual (difference between observed and predicted stomatal conductance (*g*_s)) for the survey model including a time-of-day effect.
- Fig. S7** Relationship between leaf phenological stage and photosynthetic traits.
- Fig. S8** Simulations of daily canopy transpiration (*E*) by species when using different leaf phenology distributions.
- Fig. S9** Comparison of fitted values of stomatal slope (*g*₁) and stomatal intercept (*g*₀) by species for curves conducted at different times of day.
- Fig. S10** Estimated stomatal slope (*g*₁) vs length of response curve measurement.
- Fig. S11** Stomatal slope (*g*₁) as estimated from response curves collected with decreasing (saturating to 0 μmol PAR) and increasing (0 μmol PAR to saturating) levels of irradiance.
- Fig. S12** Observed vs predicted stomatal conductance (*g*_s) from the calibration phase of model development.
- Fig. S13** Range and distribution of individual observations of leaf-level conditions collected during survey gas exchange.
- Fig. S14** Mean estimated intercellular carbon mole fraction (*C*_i) by species and leaf age.
- Fig. S15** Conceptual illustration of the link between stomatal slope and water use efficiency.
- Fig. S16** Observed vs predicted stomatal conductance (*g*_s) when a leaf water potential (Ψ_{leaf}) penalty is applied (upper panels) and when no penalty is applied (lower panels).

Supporting Information

Additional Supporting Information may be found online in the Supporting Information section at the end of the article.

Notes S1 Description of mixed effects models and their parameter estimates.

Notes S2 Description of the leaf scale photosynthesis, conductance, and energy balance model from the R package LEAFGASEXCHANGE (Lamour & Serbin, 2021).

Notes S3 Description of the leaf water potential (Ψ_{leaf}) penalty function introduced by Wolf *et al.* (2016) and tested by Anderegg *et al.* (2017).

Table S1 Parameter estimates and their standard error for the response curve model.

Table S2 Parameter estimates and their standard error for the survey model.

Table S3 Parameter estimates and their standard error for the survey + time-of-day model.

Table S4 Species-specific Weibull function values corresponding to xylem conductivity vs stem water potential (Ψ_{stem}).

Please note: Wiley is not responsible for the content or functionality of any Supporting Information supplied by the authors. Any queries (other than missing material) should be directed to the *New Phytologist* Central Office.